

[Click here to view linked References](#)

1 Convergent Evolution in Two Bacterial Replicative Helicase Loaders

2

3 Jillian Chase^{1,2}, James Berger^{3#}, and David Jeruzalmi^{1,2,4,5#}

4 ¹Department of Chemistry and Biochemistry, City College of New York, New York,
5 NY 10031, USA;

6 ³Department of Biophysics and Biophysical Chemistry, Johns Hopkins School of
7 Medicine, Baltimore, MD 21205

8 Ph.D. Programs in Biochemistry², Biology⁴, and Chemistry⁵, The Graduate Center
9 of the City University of New York, New York, NY 10016, USA;

10 #Correspondence: dj@ccny.cuny.edu (Jeruzalmi, D) or jmberger@jhmi.edu
11 (Berger, J)

12 **Abstract (120 words)**

13 Dedicated loader proteins play essential roles in bacterial DNA replication by
14 opening ring-shaped DnaB-family helicases and chaperoning ssDNA into a central motor
15 chamber as a prelude to DNA unwinding. Although unrelated in sequence, the *E. coli*
16 DnaC and bacteriophage λ P loaders feature a similar overall architecture: a globular
17 domain linked to an extended lasso/grappling hook element, located at their amino and
18 carboxy termini, respectively. Both loaders remodel a closed DnaB ring into nearly
19 identical right-handed open conformations. The sole element shared by the loaders is a
20 single alpha helix, which binds to the same site on the helicase. Physical features of the
21 loaders establish that DnaC and λ P evolved independently to converge, through
22 molecular mimicry, on a common helicase opening mechanism.

23

24 **Keywords**

25 DnaB, DnaC, λ P, DciA, DNA Replication, helicase loading, convergent evolution,
26 molecular mimicry.

27

28 **Introduction (~3100 words)**

29 **Specialized Factors Load the DnaB Bacterial Replicative Helicase onto the**
30 **Replication Origin**

31 The regulated loading of ring-shaped hexameric helicases onto chromosomal
32 origins is an essential feature of DNA replication in all cellular domains of life [1–3].
33 Helicase deposition requires specialized factors known as helicase loaders, which
34 operate during the initiation of DNA replication [4–8]. In bacteria, several helicase loaders
35 have been studied, including *Escherichia coli* (*E. coli*) DnaC [4], bacteriophage λ P,
36 *Bacillus subtilis* (*B. subtilis*) Dnal [5], and DciA/DopE, a recently described class of
37 proteins which appear in bacteria that lack orthologs of DnaC or Dnal [6,7,9]. Helicase
38 loading is also critical to assembly of eukaryal and archaeal **replisomes** [1,2,8].

39 The assembly of the bacterial replicative helicase (**Figure 1**), which is known as
40 DnaB in most bacteria or DnaC in *B. subtilis* (henceforth called DnaB), onto origin DNA
41 occurs during the initiation phase of DNA replication [8,10–14]. Our view of replication
42 initiation in bacteria is informed by studies with primary and secondary chromosomes of
43 bacteria, plasmids, and phages [15–27], and have implied the involvement of four classes
44 of factors (**Table 1**): 1) a DNA sequence called a replication origin, where DNA synthesis
45 will begin [13,20,28,29], 2) a replication initiator protein (*E. coli*: DnaA [10,12,30–32], *V.*
46 *cholerae*: DnaA, RctB [18,21,23,25,33–37], plasmids: RepE, Pi, TrfA [38–40], phage
47 lambda (λ): O [41–49]), 3) a DnaB-family replicative helicase [4,12–14,50], and, finally, 4)
48 a helicase loader (*E. coli*: DnaC [4,10,16,51–55], phage λ: P [43,45–48,56–59], *V.*
49 *cholerae*: DciA [6,9]). The multi-step process for initiating DNA replication begins with the
50 recognition and binding of multiple copies of the initiator protein to dsDNA sites at the

51 replication origin; once bound, initiator proteins associate into a complex protein-DNA
52 ensemble [4,10,12,19,31,60,61]. One of the outputs of the initiation phase of DNA
53 replication is the melting of an A-T rich segment of the replication origin termed the DNA
54 unwinding element (DUE) by the DnaA or the λ O initiator proteins [13,30,31], an event
55 that provides single DNA strands (ssDNA) as substrates for DnaB loading. DnaB
56 hexamers assemble into two-tiered rings formed by the amino (NTD) and carboxy-
57 terminal domains (CTD) of the helicase; a so-termed 'linker helix' element (LH) connects
58 these domains and packs against another alpha helix, termed the docking helix (DH), of
59 a neighboring DnaB subunit to give rise to a **domain-swapped oligomer** [62–64] (Figure
60 **2**). The two DnaB tiers circumscribe an internal chamber into which one of the ssDNA
61 strands from the replication origin will be loaded. One layer is formed out of six NTDs,
62 which assemble into two different 'trimer-of-dimers' configurations that display pseudo-
63 three-fold symmetry. These arrangements arise from alternative packing orientations for
64 NTD dimers, which create several types of subunit interfaces of likely varying stability
65 [62,65]. The CTD tier assembles out of six C-terminal domains (CTD) of DnaB, each of
66 which harbors a **RecA-like ATPase domain**. In contrast to the NTD, the CTD layer
67 exhibits a pseudo-six-fold arrangement, with a single type of interface.

68 Helicase loading onto ssDNA can be conceptually divided into four stages (Figure
69 **1**). During assembly, DnaB transitions between three conformations: closed planar, open
70 right-handed spiral, and closed right-handed spiral [62–68]. In addition, the NTD and
71 CTD layers of each of these conformers are found in one of two arrangements: dilated or
72 constricted (**Figures 2A-2B**); these conformers differ on inter-protomer contacts. The
73 isolated hexameric helicase, in both dilated and constricted closed-planar configurations,

74 populates Stage I. Formation of the helicase•helicase loader complex leads to Stage II,
75 while engagement of the helicase•loader complex with origin-derived ssDNA•initiator
76 (DnaA or λ O) populates Stage III. The ATPase and ssDNA translocation activities of the
77 helicase are suppressed during these latter two stages [56,58,69–71], with **the**
78 **DnaA/replication origin complex** also playing a role in loading or positioning the
79 **helicase/loader complex** using direct contacts between DnaA and DnaB [69–71] (the
80 **involvement of contacts between other bacterial replication initiators and DnaB** remains
81 **to be clarified**). Recently, cryogenic electron microscopy (cryo-EM) analyses of two
82 distinct bacterial helicase•loader complexes (*E. coli* DnaB•DnaC and *E. coli* DnaB• λ P,
83 **Figure 1: Stages II-III, and Figure 3**) have shown that the helicase adopts an open right-
84 handed spiral configuration, promoted, and stabilized by interactions with the helicase
85 loaders [65,68]. The transition to Stage IV is accompanied by eviction of the loader and
86 initiator from the complex on DNA, which relieves inhibition of DnaB's activities. Notably,
87 in Stage III, the configuration of the DnaB-bound loader is nearly identical to the closed
88 spiral form seen in the loader-free helicase of Stage IV [65,67].

89 Helicase loading in bacteria occurs by one of at least two reported mechanisms
90 [72], termed: a) ring breaking, where DnaB hexamers are physically opened [73], and b)
91 ring making, in which hexamers are assembled [5]. It is now clear that both *E. coli* DnaC
92 and phage λ P are ring breakers: each loader binds to and delivers a pre-formed helicase
93 hexamer to its cognate origin [4,43,45–47,56,58,74]. DnaC and λ P are similar in that
94 both are essential for their respective organisms and both bind to ssDNA [56,58,75–77].
95 λ P also can displace DnaC from *E. coli* DnaB, implying that their respective binding sites
96 overlap [58,74]. These congruencies might imply a common ancestry; however, DnaC

97 and λ P are unrelated in sequence and enzymatic function (e.g., DnaC is a known ATPase
98 [10,53,75–77], whereas λ P is not [78]). Moreover, although each loading system requires
99 ejection of the loader from the DNA complex for DnaB to transition to the translocation-
100 competent form, eviction occurs by distinct mechanisms. For DnaC, nucleotide dynamics
101 in its **AAA+ ATPase domain**, along with RNA synthesis by the DnaG primase, are
102 significant features in eviction [10,52,53,76,77,79]. By contrast, removal of λ P requires
103 the host DnaK/DnaJ/GrpE chaperone machinery [31–34]. **Helicase loading is also a**
104 **feature during restart of DNA replication after it has prematurely been halted in response**
105 **to DNA damage and involves a distinct set of proteins (PriA, PriB, PriC, and DnaT); the**
106 **reader is referred to the literature for a more complete treatment of helicase loading during**
107 **replication restart [80–82].**

108 Here, we compare recent structures of two bacterial helicase loaders: *E. coli* DnaC
109 [65] and phage λ P [68] bound to the same *E. coli* DnaB helicase (**Figure 3**). This
110 comparison provides an opportunity to understand the mechanisms of the two loaders
111 and to extract central principles associated with DnaB opening and loading onto ssDNA.
112 A recent crystal structure of the interaction domains of DnaB and DnaC [83] comports
113 with the EM analyses of the complete complexes. A new study of DciA•DnaB interactions
114 also points to some conserved elements of helicase opening in this system as well [9].
115 **Further study will be required to establish the mechanistic relationships, if any, between**
116 **the DciA and *B. subtilis* DnaI/DnaB/DnaD loaders [5,84,85] and the better understood *E.***
117 ***coli* DnaC [65] and λ P [68] systems.**

118

119 **Though unrelated by sequence and fold, *E. coli* DnaC and λ P exhibit analogous**
120 **global architectures**

121 Inspection of the *E. coli* DnaB•DnaC (BC) and the *E. coli* DnaB•phage λ P (BP)
122 complexes shows that the two loaders engage the carboxy-terminal (CTD) ATPase
123 surface of DnaB to form a three-layered ensemble [65,68,83]. One layer corresponds to
124 an oligomeric form of the helicase loader (hexameric for DnaC and pentameric for λ P),
125 while the second and third correspond to the NTD and CTD tiers of DnaB (**Figures 3A-**
126 **B**). **Although six copies of DnaC are present in the *E. coli* BC complex and five λ P**
127 **protomers are found in the BP assembly, the stoichiometries seen in the cryo-EM**
128 **structures do not necessarily preclude the possibility that complexes with fewer copies of**
129 **the loader might be active in supporting helicase loading.** Significantly, each loader
130 adopts a distinct and unrelated structure, yet the monomers of both exhibit a similar
131 overall architecture: a globular domain fused to an extended segment that forms a
132 lasso/grappling hook element (**Figures 3C-D**).

133 The globular domain of DnaC consists of an AAA+ ATPase module that is fused
134 to a ~75 residue N-terminal segment (**Figure 3C**)[65,83]. The amino-terminal segment
135 of DnaC consists of a long α-helix that extends along the CTD of a DnaB protomer and
136 initiates from a helix-loop-helix element that packs against the LH linker helix from one
137 DnaB subunit and the DH docking helix from another. Notably, the N-terminal segment
138 provides the only contacts between DnaC and the DnaB helicase. The six copies of the
139 globular DnaC AAA+ domain assemble into an open spiral like that seen in related
140 ATPases such as DnaA and archaeal/eukaryal MCM helicases [86–92]. In the absence
141 of ssDNA, five of the six nucleotide-binding sites in DnaC are populated with an ATP

142 analog (ADP•BeF₃), whereas the sixth (which sits at the gap in the DnaC spiral) engages
143 ADP, likely because its catalytic center lacks important functional contacts from a
144 neighboring protomer. Rationalizing this arrangement of nucleotides is the prior finding
145 that the ATP form of DnaC suppresses DnaB's helicase activity and as it stabilizes the
146 ssDNA complex [52].

147 For the λ P loader, only the C-terminal ~125 residues were resolved in EM density
148 maps [68]. This region consists of an α-helical globular domain fused to an extended
149 segment of ~45 residues (Figure 3D). The λ P extension forms a sub-structure
150 analogous to, but distinct from, that seen in DnaC [65,83], terminating in a single α-helix
151 that packs against the LH and DH elements of two adjacent subunits of DnaB. Both the
152 globular domain and the grappling hook/lasso segment of λ P contact two consecutive
153 subunits of the DnaB hexamer. These interactions are repeated in the five copies of λ P
154 in the BP complex to create an open helical arrangement of loaders; the breached
155 interface of the DnaB hexamer precludes binding of a sixth copy of λ P. The low resolution
156 (4.1 Å) of the BP EM maps in the region of the loader limits analysis of interfaces between
157 λ P protomers; nevertheless, an extensive interface between the five λ P protomers does
158 not appear to form.

159

160 *E. coli* DnaC and phage λP reconfigure DnaB into an open right-handed spiral

161 Despite their evolutionarily distinct structures and contacts with DnaB, both DnaC
162 and λ P reconfigure the helicase into highly similar, open-spiral configurations (root mean
163 square deviation (RMSD) of ~2.2 Å, calculated from 2611 C_α positions that span the

164 DnaB hexamer) [65,68]. The DnaB NTDs also both adopt a constricted configuration,
165 albeit with a spiral (as opposed to planar) shape that bears a split between one of the
166 subunit interfaces. The similarity between DnaB in the two loader complexes is also
167 evident from the average helical pitch and twist values of the open spirals in both the NTD
168 (~2.8 Å and 60.0° for BC vs. ~2.6 Å and 59.9° for BP) and CTD layers (~19.3 Å and
169 ~55.3° for BC vs. ~16 Å and ~56° for BP). Changes induced by each loader rupture one
170 of the DnaB subunit interfaces at both the NTD and CTD layers to create openings (15-
171 20 Å) of sufficient size to allow ssDNA access to the internal chamber.

172 Changes to the helical pitch and twist of the DnaB hexamer within each loader
173 complex combine to alter the configuration of the ssDNA-binding site in the helicase.
174 Superposition of DnaB from each loader complex reveals significant changes in the
175 position of DNA binding residues in comparison to that when DnaB is bound to ssDNA
176 (**Figure 4**) [65]. When bound to ssDNA and the loader, the CTD of each DnaB protomer
177 projects three residues (*E. coli*: R403, E404, G406) on a DNA binding loop into the
178 helicase pore to contact ssDNA. In the loader-only complexes, reconfiguration of the
179 CTD layer shifts the positions of the alpha-carbons of these residues by ~10-30 Å (in BC)
180 or ~5-20 Å (in BP).

181 The disposition and nucleotide occupancy of the six RecA-type ATPase sites in
182 DnaB are also altered in the complexes with DnaC and λ P [65,68]. ATPase activity by
183 DnaB relies on ‘composite’ nucleotide binding sites, wherein residues from two adjacent
184 subunits contribute to a single catalytic center [63,64,67,93]. In both helicase•loader
185 complexes, five of the six ATPase sites in DnaB are occupied by ADP, while the sixth,
186 which sits at the breach in the CTD ring, is vacant; when bound to just ssDNA, this

187 constellation of sites are filled with a nucleoside triphosphate analog (ADP•BeF₃) instead.
188 The alterations in CTD orientation appear to have remodeled the five ADP-filled sites of
189 the loader-bound helicase into non-optimal catalytic configurations as well, although the
190 resolution of the structures prevents a more precise evaluation of these changes [65,68].

191

192 **Two distinct helicase loader complexes with a shared function**

193 The BC and BP complexes reveal how the evolutionarily distinct structural
194 elements of DnaC and λ P converged on a common helicase-opening strategy [65,68].
195 In both loader complexes, the lasso/grappling hook segments of DnaC and λ P provide
196 key contacts to opening the DnaB helicase (**Figure 5**). Superposition of the two
197 complexes on a DnaB monomer reveals that the only segment in common between the
198 two loaders is a single α helix at the extreme amino-terminus of DnaC, or the carboxy-
199 terminus of λ P. In both complexes, this helix disrupts interactions between the LH linker
200 helix of one DnaB protomer and the DH docking helix on an adjacent subunit; each DnaB
201 protomer undergoes this interaction save for the one at the breach in the spiral. Insertion
202 of the loader α helix between the DnaB LH and DH elements reconfigures the CTD, and
203 concomitantly the NTD, tiers, from the closed planar to the open spiral form to allow
204 ssDNA to access the internal chamber of DnaB. Notably, in the BC structure, the N-
205 terminal lasso/grappling hook element represents the sole point of contact between DnaC
206 and DnaB; indeed, the isolated region harbors significant capacity to promote helicase
207 loading [66].

208 It was surprising to find that the AAA+ ATPase domains of DnaC make no contact
209 with DnaB, and thus, play no direct role in helicase opening (**Figure 3A**)[65]. By
210 comparison, the AAA+ ATPases of the evolutionarily related clamp loaders – which open
211 and chaperone the ring-shaped β and PCNA proteins onto DNA to aid polymerase
212 processivity – engage their client clamps directly [94–98]. For DnaC, the ATPase
213 elements appear to play a role in sensing the binding of ssDNA to the helicase and in
214 enhancing the efficiency of the DnaB-opening reaction [66]. **AAA+ ATPases are often**
215 **pre-formed oligomers** [99,100], unusually, in solution, DnaC is monomeric [54], however,
216 **six copies oligomerize on DnaB in a manner stabilized by ATP** [54,65]. Without ssDNA,
217 the nucleotide-binding sites of DnaC in the BC complex are filled with ATP and captured
218 in a configuration that is poised, but sub-optimal for catalysis. After sensing ssDNA, the
219 nucleotides sites on the DnaC oligomer are filled with ADP, as would be expected
220 following hydrolysis. ATP hydrolysis after ssDNA loading does not appear to allow DnaC
221 to dissociate from DnaB but may diminish stability of the DnaC oligomer. Biochemical
222 studies suggest that DnaG recruitment and primer synthesis are needed to promote loss
223 of DnaC from the complex [55,74,101].

224 In contrast to the modest interface between helicase and loader in the BC complex
225 [65,68], λ P forms an extensive interface with DnaB that encompasses both the globular
226 and lasso/grappling hook segments (**Figure 3B**). λ P is also a monomer in solution and
227 five copies assemble onto DnaB in the BP loader complex [68], however, few contacts
228 between loader subunits are seen. Inspection of the two loader complexes indicate that
229 the positioning of their C-terminal α helices between DnaB's LH and DH elements may
230 be sufficient for opening and that an extensive interface is dispensable for helicase

231 opening. This has been confirmed for DnaC [66], and we speculate that the extensive
232 interface between the DnaB and the globular domain of λ P may form because of
233 interacting with the opened helicase, rather than as its driver as previously proposed [68].
234 If so, then, what might be the functional role(s) for the extensive interface between λ P
235 and DnaB? Biochemical studies provide a potential explanation for the structural
236 dichotomy. It is known that λ P can displace DnaC from a preformed BC complex [58];
237 the extensive interface in the BP complex may aid displacement as part of a biological
238 strategy to appropriate the host replication machinery away from the bacterial
239 chromosome and toward the phage genome. Alternatively, the extensive interface in the
240 BP complex may serve as a functional analogue to the extensive AAA+ interaction
241 between DnaC globular domains in the BC complex. Regardless, in both the BC and BP
242 complexes, overall stability is achieved by oligomerization, but by distinct means [65,68].

243 Although they feature some global architectural parallels, neither the globular
244 domains of DnaC and λ P nor the extended lasso/grappling hook regions display any
245 similarity in sequence [65,68]. Underscoring the dissimilarity is the opposing chain
246 polarity of the grappling hook segments as they run across the surface of DnaB: DnaC
247 runs N-to-C whereas λ P runs C-to-N (**Figures 3C-3D and Figure 5**). The finding that a
248 single functionally significant α -helix in DnaC and λ P exhibits a divergent protein chain
249 direction confirms their lack of evolutionary kinship and instead reflects a form of
250 **molecular mimicry** that arose through **convergent evolution**. Molecular mimicry in
251 bacterial DNA replication initiation joins other examples from protein synthesis [102–104],
252 gene expression [105], apoptosis [106], host pathogen interactions [107–109], virally
253 encoded proteins[110], and immunity and autoimmunity [111].

254

255 **A recently described protein known as DciA serves as the primary helicase loader**
256 **in bacteria that lack DnaC/Dnal**

257 Outside of DnaC and λ P, Ferat and co-workers have reported that most bacteria
258 lack homologs of DnaC (or the unrelated Dnal loader) and that helicase loading in these
259 organisms instead appears to depend on a distinct protein called DciA [6] (**Table 1**). A
260 structure of DciA from *Vibrio cholerae* (VcDciA) shows that the protein is composed of an
261 ~110 aa N-terminal globular domain followed by a ~40 aa disordered C-terminal segment.
262 Interestingly, the fold of the DciA globular domain is related to the N-terminal domain of
263 the replication initiator, DnaA, as well as the C-terminal domain of the γ/τ /DnaX clamp
264 loader subunit and the FliK flagellar hook-length control protein. VcDciA appears to
265 stimulate the loading of the VcDnaB helicase onto DNA through a DciA₃:DnaB₆
266 intermediate; the LH-DH nexus that is targeted by DnaC and λ P has been suggested to
267 serve as an important point of contact in this complex as well [9]. It has been proposed
268 that VcDnaB may adopt an open spiral in solution and may harbor residues that specify
269 loader preference. Given the widespread nature of the DciA system, additional chapters
270 of the helicase loader story clearly remain to be written.

271

272 **Concluding Remarks**

273 In all cellular organisms, the regulated association of the replicative helicase with
274 replication origins sets the stage for the initiation of DNA replication [1–8] (**Table 1** and
275 **Figure 1**). However, significant differences are now evident in mechanisms by which

276 origin unwinding and helicase loading take place in bacteria as compared to archaea and
277 eukaryotes. In bacterial replication systems, the current model holds that the initiator
278 protein not only marks an origin for initiation, but also melts that origin, enabling the
279 replicative helicase•loader complex to load onto the resultant ssDNA [8,12,13,31,112].
280 By contrast, in archaea and eukaryotes, the helicase is loaded by an initiator complex
281 around duplex DNA, which is then subsequently melted by the helicase itself [113–118].
282 These distinct mechanisms are remarkable given that replication initiation machinery in
283 all three domains of life is predicated on a related AAA+ fold [8,13,86]. Why the two
284 approaches arose during evolution is unclear but may reflect an adaption to the two
285 different families of hexameric helicases – one based on a RecA ATPase fold, and
286 another based on a AAA+ ATPase domain [119–123] – that have been employed to
287 support replication in bacteria as compared to archaea and eukaryotes. Structural
288 analyses of two bacterial loaders bound to the *E. coli* DnaB helicase have for the first time
289 illuminated the rich detail and diversity of helicase-ring opening as well as DNA
290 association (**Figures 2, 3, 4 and Figure 5**). However, despite the insights gained from
291 these models, several fundamental questions about replication initiation and helicase
292 loading remain to be addressed (Outstanding Questions).

293

422 **Acknowledgements**

423 This work was supported by the National Science Foundation (DJ: MCB 1818255),
424 the National Institutes of Health (DJ: R-01-GM084162 JMB: R37-071747), and the
425 Department of Education (JC: PA200A150068).

426

427 **Tables, Figures, and Figure legends**

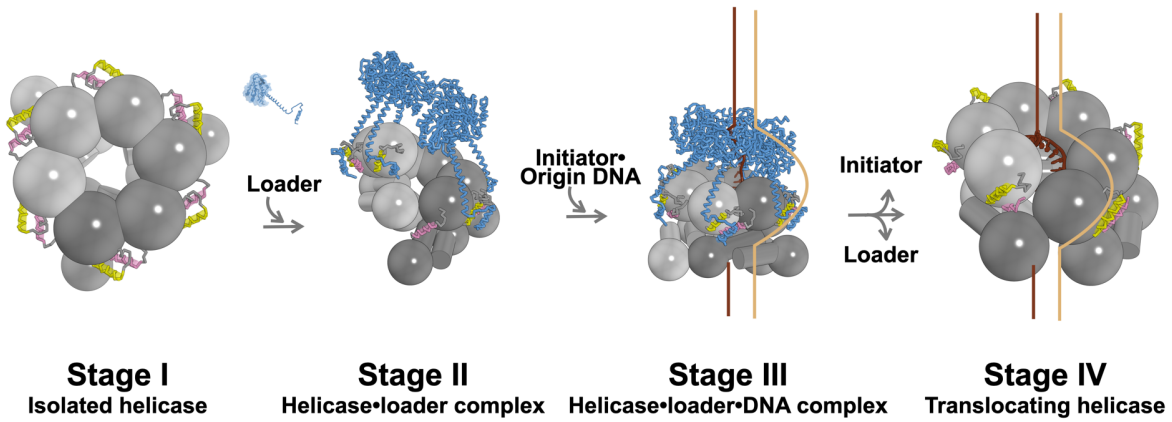
428

429

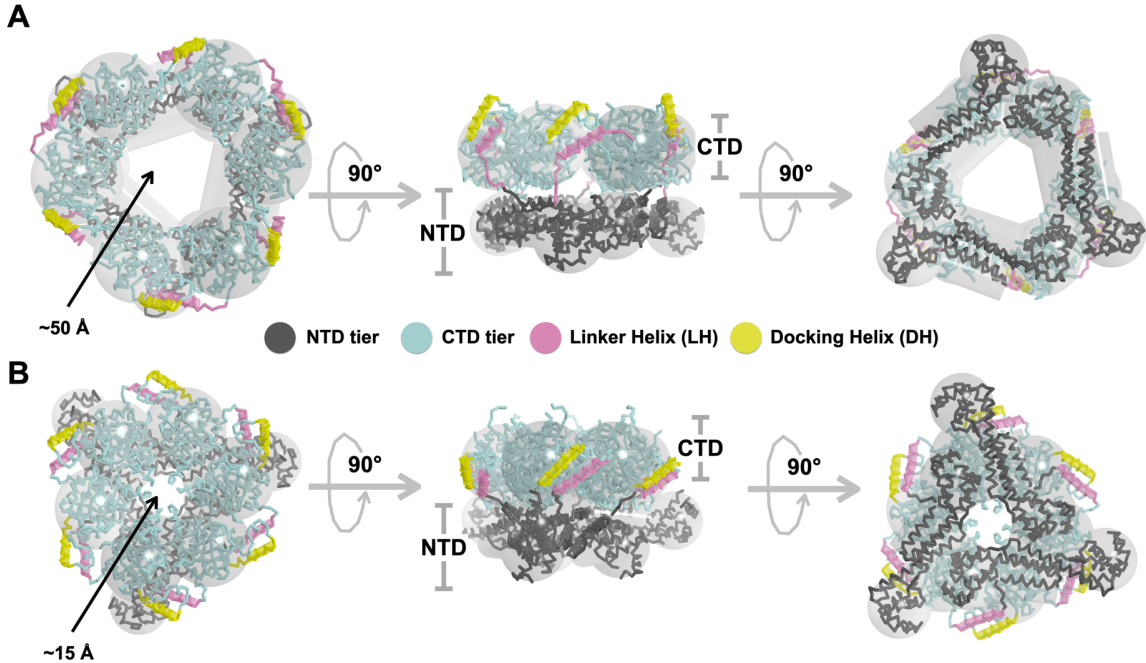
	<i>E. coli</i>	phage λ	<i>V. cholerae</i>
origin DNA	OriC	Oriλ	OriC-I/II
initiator	DnaA	O	DnaA/RctB
helicase	DnaB	DnaB	DnaB
loader	DnaC	P	DciA

430 **Table 1.** Molecules involved in various bacterial DNA replication initiation systems.
431

432



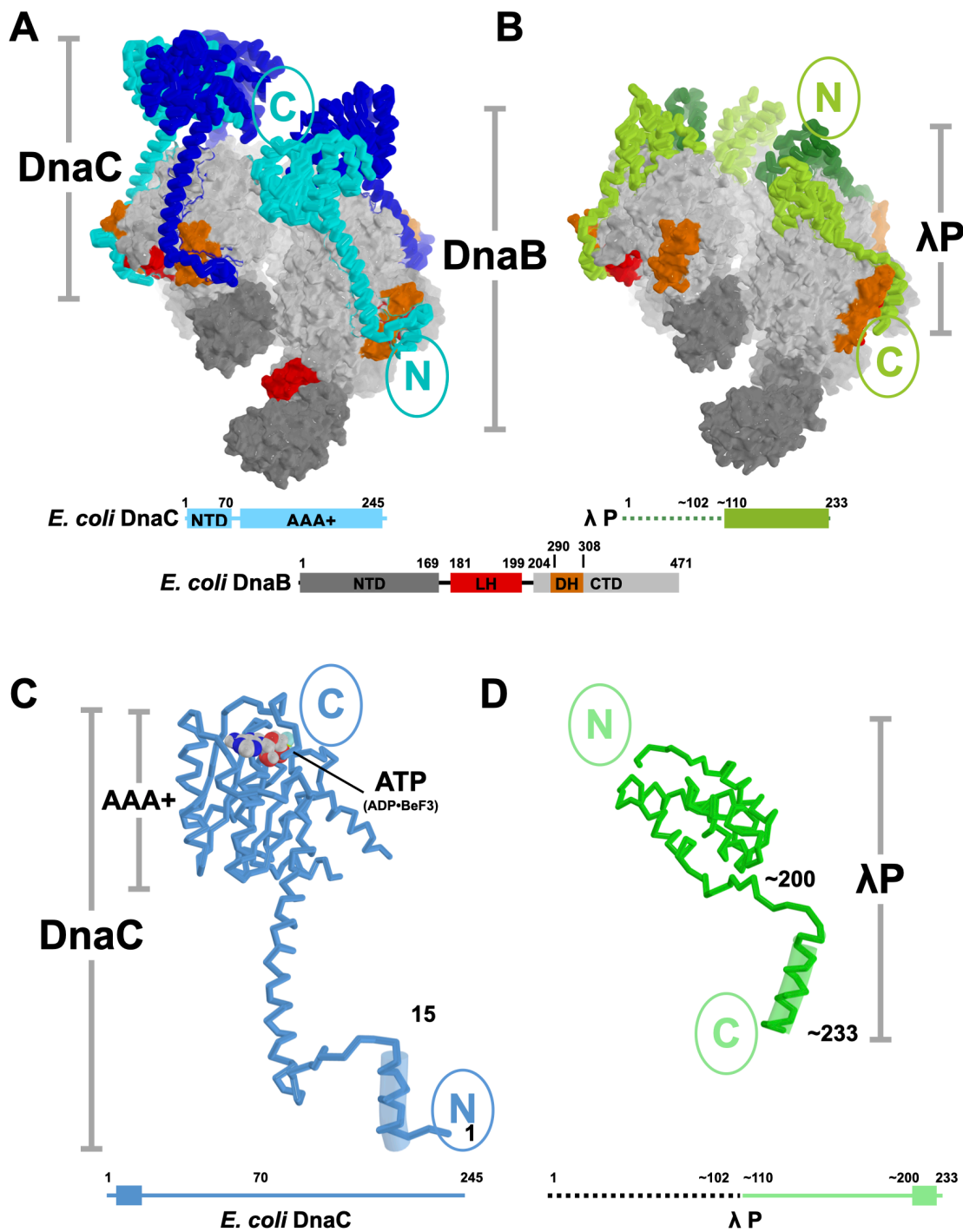
433
 434 **Figure 1. Loading of the Bacterial DnaB Replicative Helicase at a Replication Origin.**
 435 The DnaB loading pathway passes through at least four stages (I, II, III, and IV). DnaB
 436 sub-domains are depicted according to their overall shape (amino-terminal domain
 437 (NTD): a mushroom-like shape; carboxy-terminal domain (CTD): sphere; both in varying
 438 shades of gray). The Linker-Helix (LH, pink) and Docking-Helix (DH, yellow) elements
 439 are depicted in a ribbon and transparent cylinder representation. The DnaC helicase
 440 loader is shown as a blue ribbon. The DNA strands, one of which is included in the
 441 central DnaB chamber, and the second excluded, are colored in chocolate brown and
 442 light brown, respectively.
 443
 444
 445
 446
 447
 448



449

450 **Figure 2. Overview of the DnaB replicative helicase.** DnaB adopts at least two distinct
 451 configurations, termed dilated (A) and constricted (B) [62–64]. DnaB sub-domains are
 452 depicted according to their overall shape (amino-terminal domain (NTD): a mushroom-
 453 like shape; carboxy-terminal domain (CTD): sphere; both in varying shades of gray).
 454 Superimposed on these shapes of DnaB are ribbon representations, colored in gray and
 455 light cyan of the NTD and CTD tiers, respectively, in various poses of the dilated (A, PDB
 456 = 2R6A) and constricted (B, PDB = 4NMN) forms of DnaB. The linker and docking helices
 457 are depicted as cylinders, and colored pink and yellow, respectively.

458



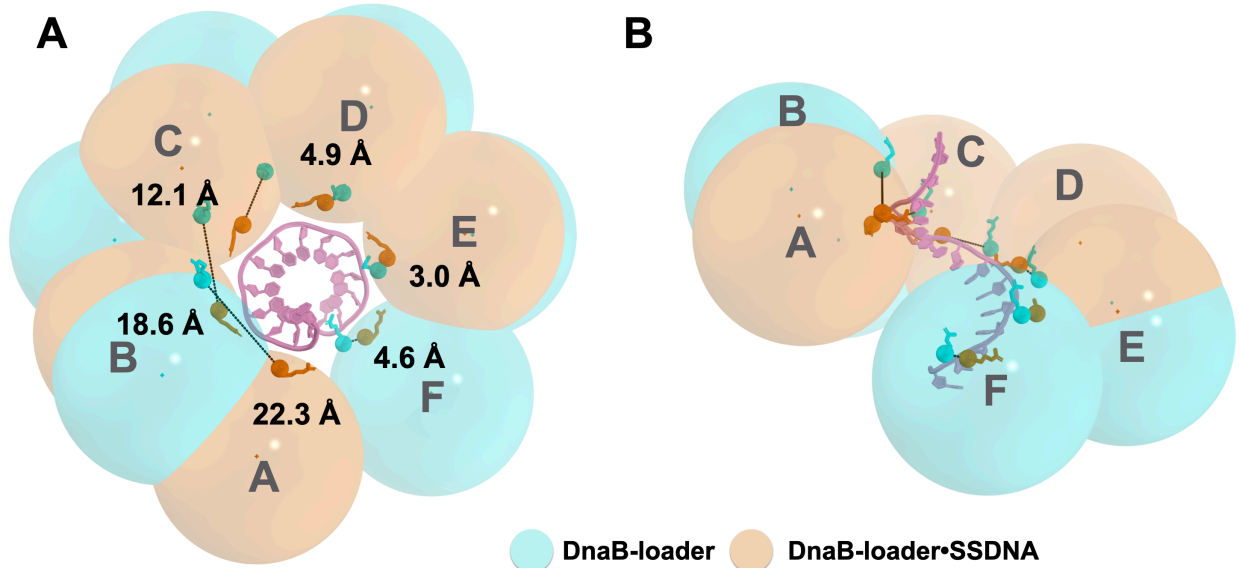
459
460
461
462
463
464

Figure 3. *E. coli* DnaB Complexed with the DnaC (A) and λ P (B) Helicase Loaders.
 Protomers of the DnaC and λ P helicase loaders are colored in alternating shades of blue (DnaC) and green (λ P). The *E. coli* DnaB helicase in each loader complex is represented in a surface rendering, with the amino-terminal domain (NTD) and the carboxy-terminal domain (CTD) layers colored in darker and lighter shades of gray, respectively. Linker-

465 helices (LH) and docking-helices (DH) are in colored in red and orange, respectively. The
466 DnaB hexamers from the loader complexes are superimposed on the CTD of the
467 protomer at the bottom of the spiral in this pose. The primary sequence of each loader
468 and DnaB is represented as a linear schematic, with salient features annotated and
469 colored to match the molecular representations. Only the carboxy terminal domain of λ
470 P was visible in the EM maps of the BP complex (the missing segment is depicted as a
471 dashed line). The terminal helix of each loader (DnaC: N-terminal; λ P: C-terminal) are
472 depicted as ribbons and transparent cylinders. The amino (N) and carboxy (C) termini of
473 each loader is indicated in each panel.

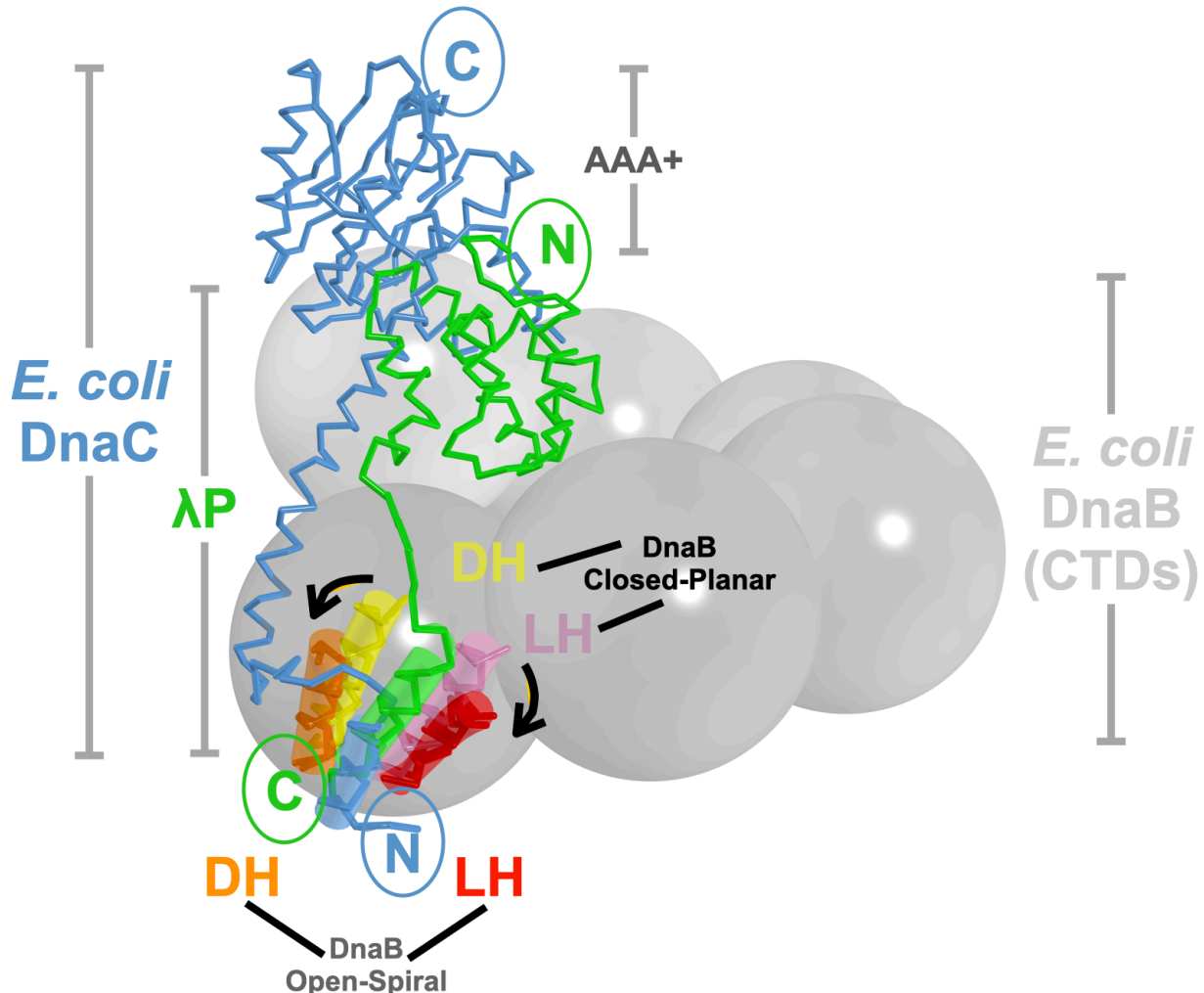
474

475



476
 477 **Figure 4. The ssDNA Binding Site is Altered in the Loader Bound Form of DnaB.**
 478 The BC complex without ssDNA (PDB = 6QEL) was superimposed (RMSD = 0.85 Å) onto
 479 the C-terminal domain of chain F of the ssDNA bound complex (PDB = 6QEM). The large
 480 spheres represent the CTDs of the BC complex with (light brown) and without (cyan)
 481 ssDNA. The alpha carbons of arginine 403, which makes a key contact to ssDNA in the
 482 BC complex, are depicted as smaller spheres for the ssDNA complex (brown) and apo
 483 complex (dark cyan). Distances between the alpha carbons of arginine 403 from
 484 equivalent DnaB subunits are shown. The six chains from the ssDNA-bound complex
 485 are identified by letters (A, B, C, etc.). Poses in panels A and B are related by a 90°
 486 rotation about the horizontal axis.

487
 488



489
490 **Figure 5. Convergent Evolution/Molecular Mimicry in the Mechanism of Opening**
491 **of the *E. coli* DnaB Replicative Helicase by the *E. coli* DnaC and λ P Helicase**
492 **Loaders.** The DnaC and λ P helicase loaders are shown in a ribbon representation,

493 colored light blue (DnaC) and green (λ P), with their respective amino and carboxy termini
494 marked. For clarity, only one copy of each loader is shown. The DnaB hexamer from
495 each loader complex is superimposed on the carboxy-terminal domain (CTD) of the
496 protomer at the bottom of the spiral in this pose; the docking helix element was excluded
497 from the alignment to produce an RMSD of 1.3 Å. For clarity, only the CTD tier of DnaB,
498 represented as a set of spheres, colored in varying shades of gray, is shown. The linker
499 (LH) and docking (DH) helices are depicted as a ribbon and transparent cylinder. The LH
500 and DH from the closed-planar form of DnaB are colored yellow and pink, respectively;
501 the corresponding elements from the DnaC and λ P loader-bound DnaB are in orange
502 and red, respectively. The black arrow signifies direction of motion of the LH and DH
503 elements on binding the DnaC and λ P loaders.

504

505 **References**

506

- 507 1 Yao, N. and O'Donnell, M. (2016) Bacterial and Eukaryotic Replisome Machines. *JSM*
508 *biochemistry and molecular biology* 3,
- 509 2 Yao, N.Y. and O'Donnell, M.E. (2016) Evolution of replication machines. *Critical*
510 *Reviews in Biochemistry and Molecular Biology* 51, 135–149
- 511 3 MacNeill, S.A. (2011) Protein-protein interactions in the archaeal core replisome.
512 *Biochemical Society transactions* 39, 163–168
- 513 4 Kaguni, J.M. (2014) DnaA, DnaB, and DnaC. pp. 1–14, Springer New York
- 514 5 Velten, M. et al. (2003) A Two-Protein Strategy for the Functional Loading of a
515 Cellular Replicative DNA Helicase. *Mol Cell* 11, 1009–1020
- 516 6 Brézellec, P. et al. (2016) DciA is an ancestral replicative helicase operator essential
517 for bacterial replication initiation. *Nature communications* 7, 13271
- 518 7 Brézellec, P. et al. (2017) Domestication of lambda phage genes into a putative third
519 type of Replicative Helicase Matchmaker. *Genome Biology and Evolution* 9, 1561–1566
- 520 8 Bleichert, F. et al. (2017) Mechanisms for initiating cellular DNA replication. *Science*
521 355, eaah6317
- 522 9 Marsin, S. et al. (2021) Study of the DnaB:DciA interplay reveals insights into the
523 primary mode of loading of the bacterial replicative helicase. *Nucleic Acids Res* DOI:
524 10.1093/nar/gkab463
- 525 10 Bell, S.P. and Kaguni, J.M. (2013) Helicase loading at chromosomal origins of
526 replication. *Cold Spring Harbor perspectives in biology* 5, a010124
- 527 11 Kaguni, J.M. (2013) DNA Replication: Initiation in Bacteria. pp. 121–125, Elsevier
- 528 12 Chodavarapu, S. and Kaguni, J.M. (2016) Replication Initiation in Bacteria. 39, 1–30
- 529 13 Katayama, T. (2017) Initiation of DNA Replication at the Chromosomal Origin of E.
530 *coli*, *oriC*. *Adv Exp Med Biol* 1042, 79–98
- 531 14 Lewis, J.S. et al. (2016) The *E. coli* DNA Replication Fork. *The Enzymes* 39, 31–88
- 532 15 Mott, M.L. and Berger, J.M. (2007) DNA replication initiation: mechanisms and
533 regulation in bacteria. *Nature Reviews Microbiology* 5, 343–354

- 534 16 Duderstadt, K.E. et al. (2010) Origin remodeling and opening in bacteria rely on
535 distinct assembly states of the DnaA initiator. *The Journal of biological chemistry* 285,
536 28229–28239
- 537 17 Egan, E.S. and Waldor, M.K. (2003) Distinct Replication Requirements for the Two
538 *Vibrio cholerae* Chromosomes. *Cell* 114, 521–530
- 539 18 Orlova, N. et al. (2017) The replication initiator of the cholera pathogen's second
540 chromosome shows structural similarity to plasmid initiators. *Nucleic Acids Res* 45,
541 3724–3737
- 542 19 Leonard, A.C. and Grimwade, J.E. (2015) The oriSome: structure and function. *Front*
543 *Microbiol* 6, 545
- 544 20 Wolański, M. et al. (2014) oriC-encoded instructions for the initiation of bacterial
545 chromosome replication. *Frontiers in microbiology* 5, 735
- 546 21 Val, M.E. et al. (2016) A checkpoint control orchestrates the replication of the two
547 chromosomes of *Vibrio cholerae*. *Science Advances* 2, e1501914–e1501914
- 548 22 Val, M.-E. et al. (2014) Management of multipartite genomes: the *Vibrio cholerae*
549 model. *Current Opinion in Microbiology* 22, 120–126
- 550 23 Gerding, M.A. et al. (2015) Molecular Dissection of the Essential Features of the
551 Origin of Replication of the Second *Vibrio cholerae* Chromosome. *mBio* 6,
- 552 24 Fournes, F. et al. (2018) Replicate Once Per Cell Cycle: Replication Control of
553 Secondary Chromosomes. *Frontiers in microbiology* 9, 1833
- 554 25 Martins, F. de L. et al. (2018) *Vibrio cholerae* chromosome 2 copy number is
555 controlled by the methylation-independent binding of its monomeric initiator to the
556 chromosome 1 crtS site. *Nucleic Acids Research* 81, e00019-17–12
- 557 26 Konieczny, I. et al. (2014) Iteron Plasmids. *Microbiology Spectrum* 2,
- 558 27 Weigel, C. and Seitz, H. (2006) Bacteriophage replication modules. *FEMS*
559 *microbiology reviews* 30, 321–381
- 560 28 Trojanowski, D. et al. (2018) Where and When Bacterial Chromosome Replication
561 Starts: A Single Cell Perspective. *Front Microbiol* 9, 2819
- 562 29 Luo, H. et al. (2018) Recent development of Ori-Finder system and DoriC database
563 for microbial replication origins. *Brief Bioinform* 20, 1114–1124
- 564 30 Kohiyama, M. (2020) Research on DnaA in the early days. *Res Microbiol* 171, 287–
565 289

- 566 31 Leonard, A.C. et al. (2019) Changing Perspectives on the Role of DnaA-ATP in
567 Orisome Function and Timing Regulation. *Front Microbiol* 10, 2009
- 568 32 Hansen, F.G. and Atlung, T. (2018) The DnaA Tale. *Front Microbiol* 9, 319
- 569 33 Egan, E.S. and Waldor, M.K. (2003) Distinct replication requirements for the two
570 *Vibrio cholerae* chromosomes. *Cell* 114, 521–530
- 571 34 Chatterjee, S. et al. (2020) Interactions of replication initiator RctB with single- and
572 double-stranded DNA in origin opening of *Vibrio cholerae* chromosome 2. *Nucleic Acids*
573 *Res* DOI: 10.1093/nar/gkaa826
- 574 35 Ramachandran, R. et al. (2018) Chromosome 1 licenses chromosome 2 replication
575 in *Vibrio cholerae* by doubling the crtS gene dosage. *PLoS genetics* 14, e1007426
- 576 36 Jha, J.K. et al. (2014) Initiator protein dimerization plays a key role in replication
577 control of *Vibrio cholerae* chromosome 2. *Nucleic Acids Research* 42, 10538–10549
- 578 37 Fournes, F. et al. (2021) The coordinated replication of *Vibrio cholerae*'s two
579 chromosomes required the acquisition of a unique domain by the RctB initiator. *Nucleic*
580 *Acids Res* 49, 11119–11133
- 581 38 Wegrzyn, K.E. et al. (2016) Replisome Assembly at Bacterial Chromosomes and
582 Iteron Plasmids. *Frontiers in molecular biosciences* 3, 617
- 583 39 Wawrzyczka, A. et al. (2015) Plasmid replication initiator interactions with origin 13-
584 mers and polymerase subunits contribute to strand-specific replisome assembly. *Proc*
585 *National Acad Sci* 112, E4188–E4196
- 586 40 Konieczny, I. et al. (2014) Iteron Plasmids. *Microbiol Spectr* 2,
- 587 41 Wickner, S. and McKenney, K. (1987) Deletion analysis of the DNA sequence
588 required for the in vitro initiation of replication of bacteriophage lambda. *The Journal of*
589 *biological chemistry* 262, 13163–13167
- 590 42 Wold, M.S. et al. (1982) Initiation of bacteriophage lambda DNA replication in vitro
591 with purified lambda replication proteins. *Proceedings of the National Academy of*
592 *Sciences of the United States of America* 79, 6176–6180
- 593 43 Alfano, C. and McMacken, R. (1989) Ordered assembly of nucleoprotein structures
594 at the bacteriophage lambda replication origin during the initiation of DNA replication.
595 *The Journal of biological chemistry* 264, 10699–10708
- 596 44 Mensa-Wilmot, K. et al. (1989) Reconstitution of a nine-protein system that initiates
597 bacteriophage lambda DNA replication. *The Journal of biological chemistry* 264, 2853–
598 2861

- 599 45 Dodson, M. et al. (1989) Specialized nucleoprotein structures at the origin of
600 replication of bacteriophage lambda. Protein association and disassociation reactions
601 responsible for localized initiation of replication. *The Journal of biological chemistry* 264,
602 10719–10725
- 603 46 Dodson, M. et al. (1985) Specialized nucleoprotein structures at the origin of
604 replication of bacteriophage lambda: complexes with lambda O protein and with lambda
605 O, lambda P, and *Escherichia coli* DnaB proteins. *Proceedings of the National Academy
606 of Sciences of the United States of America* 82, 4678–4682
- 607 47 Dodson, M. et al. (1986) Specialized nucleoprotein structures at the origin of
608 replication of bacteriophage lambda: localized unwinding of duplex DNA by a six-protein
609 reaction. *Proceedings of the National Academy of Sciences of the United States of
610 America* 83, 7638–7642
- 611 48 LeBowitz, J.H. and McMacken, R. (1984) The bacteriophage lambda O and P
612 protein initiators promote the replication of single-stranded DNA. *Nucleic Acids
613 Research* 12, 3069–3088
- 614 49 Roberts, J.D. and McMacken, R. (1983) The bacteriophage lambda O replication
615 protein: isolation and characterization of the amplified initiator. *Nucleic Acids Research*
616 11, 7435–7452
- 617 50 O'Donnell, M.E. and Li, H. (2018) The ring-shaped hexameric helicases that function
618 at DNA replication forks. *Nat Struct Mol Biol* 25, 122–130
- 619 51 Galletto, R. and Bujalowski, W. (2002) The *E. coli* replication factor DnaC protein
620 exists in two conformations with different nucleotide binding capabilities. I.
621 Determination of the binding mechanism using ATP and ADP fluorescent analogues.
622 *Biochemistry* 41, 8907–8920
- 623 52 Davey, M.J. et al. (2002) The DnaC helicase loader is a dual ATP/ADP switch
624 protein. *The EMBO journal* 21, 3148–3159
- 625 53 Mott, M.L. et al. (2008) Structural synergy and molecular crosstalk between bacterial
626 helicase loaders and replication initiators. *Cell* 135, 623–634
- 627 54 Galletto, R. et al. (2004) Global conformation of the *Escherichia coli* replication factor
628 DnaC protein in absence and presence of nucleotide cofactors. *Biochemistry* 43,
629 10988–11001
- 630 55 Felczak, M.M. et al. (2017) DnaC, the indispensable companion of DnaB helicase,
631 controls the accessibility of DnaB helicase by primase. *The Journal of biological
632 chemistry* 292, 20871–20882

- 633 56 Learn, B.A. et al. (1997) Cryptic single-stranded-DNA binding activities of the phage
634 lambda P and Escherichia coli DnaC replication initiation proteins facilitate the transfer
635 of E. coli DnaB helicase onto DNA. *Proceedings of the National Academy of Sciences*
636 of the United States of America
- 637 57 Stephens, K.M. and McMacken, R. (1997) Functional properties of replication fork
638 assemblies established by the bacteriophage lambda O and P replication proteins. *The*
639 *Journal of biological chemistry* 272, 28800–28813
- 640 58 Mallory, J.B. et al. (1990) Host virus interactions in the initiation of bacteriophage
641 lambda DNA replication. Recruitment of Escherichia coli DnaB helicase by lambda P
642 replication protein. *The Journal of biological chemistry* 265, 13297–13307
- 643 59 Alfano, C. and McMacken, R. (1989) Heat shock protein-mediated disassembly of
644 nucleoprotein structures is required for the initiation of bacteriophage lambda DNA
645 replication. *The Journal of biological chemistry* 264, 10709–10718
- 646 60 Bleichert, F. (2019) Mechanisms of replication origin licensing: a structural
647 perspective. *Curr Opin Struc Biol* 59, 195–204
- 648 61 Kaguni, J.M. (2018) The Macromolecular Machines that Duplicate the Escherichia
649 coli Chromosome as Targets for Drug Discovery. *Antibiotics* 7, 23
- 650 62 Wang, G. et al. (2008) The structure of a DnaB-family replicative helicase and its
651 interactions with primase. *Nat Struct Mol Biol* 15, 94–100
- 652 63 Strychar ska, M.S. et al. (2013) Nucleotide and partner-protein control of bacterial
653 replicative helicase structure and function. *Molecular Cell* 52, 844–854
- 654 64 Bailey, S. et al. (2007) Structure of hexameric DnaB helicase and its complex with a
655 domain of DnaG primase. *Science (New York, NY)* 318, 459–463
- 656 65 Arias-Palomo, E. et al. (2019) Physical Basis for the Loading of a Bacterial
657 Replicative Helicase onto DNA. *Mol Cell* 74, 173–184.e4
- 658 66 Arias-Palomo, E. et al. (2013) The Bacterial DnaC Helicase Loader Is a DnaB Ring
659 Breaker. *Cell* 153, 438–448
- 660 67 Itsathitphaisarn, O. et al. (2012) The hexameric helicase DnaB adopts a nonplanar
661 conformation during translocation. *Cell* 151, 267–277
- 662 68 Chase, J. et al. (2018) Mechanisms of opening and closing of the bacterial
663 replicative helicase. *Elife* 7, 1822

- 664 69 Marszalek, J. et al. (1996) Domains of DnaA protein involved in interaction with
665 DnaB protein, and in unwinding the *Escherichia coli* chromosomal origin. *The Journal of*
666 *biological chemistry* 271, 18535–18542
- 667 70 Marszalek, J. and Kaguni, J.M. (1994) DnaA protein directs the binding of DnaB
668 protein in initiation of DNA replication in *Escherichia coli*. *The Journal of biological*
669 *chemistry* 269, 4883–4890
- 670 71 Sutton, M.D. et al. (1998) *Escherichia coli* DnaA protein. The N-terminal domain and
671 loading of DnaB helicase at the *E. coli* chromosomal origin. *The Journal of biological*
672 *chemistry* 273, 34255–34262
- 673 72 Davey, M.J. and O'Donnell, M. (2003) Replicative helicase loaders: ring breakers
674 and ring makers. *Current biology* : CB 13, R594-6
- 675 73 Kornberg, A. and Baker, T.A. (2005) *DNA Replication*, University Science Books.
- 676 74 Chodavarapu, S. et al. (2015) DnaC traps DnaB as an open ring and remodels the
677 domain that binds primase. *Nucleic Acids Research* DOI: 10.1093/nar/gkv961
- 678 75 Davey, M.J. et al. (2002) Motors and switches: AAA+ machines within the replisome.
679 *Nature Reviews Molecular Cell Biology* 3, 826–835
- 680 76 Wahle, E. et al. (1989) The dnaB-dnaC replication protein complex of *Escherichia*
681 *coli*. I. Formation and properties. *The Journal of biological chemistry* 264, 2463–2468
- 682 77 Wahle, E. et al. (1989) The dnaB-dnaC replication protein complex of *Escherichia*
683 *coli*. II. Role of the complex in mobilizing dnaB functions. *The Journal of biological*
684 *chemistry* 264, 2469–2475
- 685 78 Biswas, S.B. and Biswas, E.E. (1987) Regulation of Dnab Function in Dna-
686 Replication in *Escherichia-Coli* by Dnac and Lambda-P Gene-Products. *The Journal of*
687 *biological chemistry* 262, 7831–7838
- 688 79 Puri, N. et al. (2021) The molecular coupling between substrate recognition and ATP
689 turnover in a AAA+ hexameric helicase loader. *Elife* 10, e64232
- 690 80 Sandler, S.J. (2005) Requirements for Replication Restart Proteins During
691 Constitutive Stable DNA Replication in *Escherichia coli* K-12. *Genetics* 169, 1799–1806
- 692 81 Michel, B. and Sandler, S.J. (2017) Replication Restart in Bacteria. *J Bacteriol* 199,
693 e00102-17
- 694 82 Michel, B. et al. (2018) Replication Fork Breakage and Restart in *Escherichia coli*.
695 *Microbiol Mol Biol R* 82, e00013-18

- 696 83 Nagata, K. et al. (2019) Crystal structure of the complex of the interaction domains of
697 E. coli DnaB helicase and DnaC helicase loader: Structural basis implying a distortion-
698 accumulation mechanism for the DnaB ring opening caused by DnaC binding. *Journal*
699 of *biochemistry* 5, a010108
- 700 84 Bruand, C. et al. (2005) Functional interplay between the *Bacillus subtilis* DnaD and
701 DnaB proteins essential for initiation and re-initiation of DNA replication. *Molecular*
702 *Microbiology* 55, 1138–1150
- 703 85 Ioannou, C. et al. (2006) Helicase binding to DnaI exposes a cryptic DNA-binding
704 site during helicase loading in *Bacillus subtilis*. *Nucleic Acids Research* 34, 5247–5258
- 705 86 Duderstadt, K.E. and Berger, J.M. (2013) A structural framework for replication origin
706 opening by AAA+ initiation factors. *Current Opinion in Structural Biology* 23, 144–153
- 707 87 Gates, S.N. and Martin, A. (2019) Stairway to translocation: AAA+ motor structures
708 reveal the mechanisms of ATP-dependent substrate translocation. *Protein science : a*
709 *publication of the Protein Society* DOI: 10.1002/pro.3743
- 710 88 Miller, J.M. and Enemark, E.J. (2016) Fundamental Characteristics of AAA+ Protein
711 Family Structure and Function. *Archaea* (Vancouver, BC) 2016, 9294307
- 712 89 Duderstadt, K.E. and Berger, J.M. (2008) AAA+ ATPases in the Initiation of DNA
713 Replication. *Crit Rev Biochem Mol* 43, 163–187
- 714 90 Greci, M.D. and Bell, S.D. (2020) Archaeal DNA Replication. *Annu Rev Microbiol* 74,
715 1–16
- 716 91 Kelman, L.M. et al. (2020) Unwinding 20 Years of the Archaeal Minichromosome
717 Maintenance Helicase. *J Bacteriol* 202,
- 718 92 Bai, L. et al. (2017) DNA Replication, From Old Principles to New Discoveries.
719 *Advances in experimental medicine and biology* 1042, 207–228
- 720 93 Wiegand, T. et al. (2019) The conformational changes coupling ATP hydrolysis and
721 translocation in a bacterial DnaB helicase. *Nat Commun* 10, 31
- 722 94 Kelch, B.A. (2016) Review: The lord of the rings: Structure and mechanism of the
723 sliding clamp loader. *Biopolymers* 105, 532–546
- 724 95 Kelch, B.A. et al. (2011) How a DNA polymerase clamp loader opens a sliding
725 clamp. *Science* (New York, NY) 334, 1675–1680
- 726 96 Simonetta, K.R. et al. (2009) The mechanism of ATP-dependent primer-template
727 recognition by a clamp loader complex. *Cell* 137, 659–671

- 728 97 Bowman, G.D. et al. (2004) Structural analysis of a eukaryotic sliding DNA clamp–
729 clamp loader complex. *Nature* 429, 724–730
- 730 98 Erzberger, J.P. and Berger, J.M. (2006) Evolutionary relationships and structural
731 mechanisms of AAA+ proteins. *Annual Review of Biophysics and Biomolecular
732 Structure* 35, 93–114
- 733 99 Khan, Y.A. et al. (2021) The AAA+ superfamily: a review of the structural and
734 mechanistic principles of these molecular machines. *Crit Rev Biochem Mol* DOI:
735 10.1080/10409238.2021.1979460
- 736 100 Puchades, C. et al. (2020) The molecular principles governing the activity and
737 functional diversity of AAA+ proteins. *Nat Rev Mol Cell Bio* 21, 43–58
- 738 101 Makowska-Grzyska, M. and Kaguni, J.M. (2010) Primase directs the release of
739 DnaC from DnaB. *Molecular Cell* 37, 90–101
- 740 102 Costantino, D. et al. (2008) tRNA-mRNA mimicry drives translation initiation from a
741 viral IRES. *Nature Structural & Molecular Biology* 15, 57–64
- 742 103 Ryckelynck, M. et al. (2005) tRNAs and tRNA mimics as cornerstones of
743 aminoacyl-tRNA synthetase regulations. *Biochimie* 87, 835–845
- 744 104 Nakamura, Y. and Ito, K. (2011) tRNA mimicry in translation termination and
745 beyond. *Wiley Interdisciplinary Reviews: RNA* 2, 647–668
- 746 105 Liu, D. et al. (1998) Solution structure of a TBP-TAF(II)230 complex: protein
747 mimicry of the minor groove surface of the TATA box unwound by TBP. *Cell* 94, 573–
748 583
- 749 106 Riedl, S.J. et al. (2001) Structural Basis for the Inhibition of Caspase-3 by XIAP.
750 *Cell* 104, 1–10
- 751 107 Pahari, S. et al. (2017) Morbid Sequences Suggest Molecular Mimicry between
752 Microbial Peptides and Self-Antigens: A Possibility of Inciting Autoimmunity. *Frontiers in
753 microbiology* 8, 392
- 754 108 Chemes, L.B. et al. (2015) Convergent evolution and mimicry of protein linear
755 motifs in host-pathogen interactions. *Current Opinion in Structural Biology* 32, 91–101
- 756 109 Drayman, N. et al. (2013) Pathogens Use Structural Mimicry of Native Host Ligands
757 as a Mechanism for Host Receptor Engagement. *Cell host & microbe* 14, 63–73
- 758 110 Lasso, G. et al. (2020) A Sweep of Earth’s Virome Reveals Host-Guided Viral
759 Protein Structural Mimicry and Points to Determinants of Human Disease. *Cell Syst* 12,
760 82–91.e3

- 761 111 Wucherpfennig, K.W. and Strominger, J.L. (1995) Molecular mimicry in T cell-
762 mediated autoimmunity: Viral peptides activate human T cell clones specific for myelin
763 basic protein. *Cell* 80, 695–705
- 764 112 Grimwade, J.E. and Leonard, A.C. (2021) Blocking, Bending, and Binding:
765 Regulation of Initiation of Chromosome Replication During the *Escherichia coli* Cell
766 Cycle by Transcriptional Modulators That Interact With Origin DNA. *Front Microbiol* 12,
767 732270
- 768 113 Zhai, Y. and Tye, B.-K. (2017) Structure of the MCM2-7 Double Hexamer and Its
769 Implications for the Mechanistic Functions of the Mcm2-7 Complex. *Adv Exp Med Biol*
770 1042, 189–205
- 771 114 Fernandez, A.J. and Berger, J.M. (2021) Mechanisms of hexameric helicases. *Crit
772 Rev Biochem Mol* DOI: 10.1080/10409238.2021.1954597
- 773 115 Yuan, Z. et al. (2020) Structural mechanism of helicase loading onto replication
774 origin DNA by ORC-Cdc6. *Proc National Acad Sci* DOI: 10.1073/pnas.2006231117
- 775 116 Yuan, Z. et al. (2020) DNA unwinding mechanism of a eukaryotic replicative CMG
776 helicase. *Nat Commun* 11, 688
- 777 117 Langston, L.D. and O'Donnell, M.E. (2019) An explanation for origin unwinding in
778 eukaryotes. *Elife* 8, e46515
- 779 118 Yuan, Z. et al. (2018) Structure of Eukaryotic CMG Helicase at a Replication Fork
780 and Implications for Replisome Architecture and Origin Initiation. *Faseb J* 32, 646.7-
781 646.7
- 782 119 Koonin, E.V. (1993) A common set of conserved motifs in a vast variety of putative
783 nucleic acid-dependent ATPases including MCM proteins involved in the initiation of
784 eukaryotic DNA replication. *Nucleic Acids Research* 21, 2541–2547
- 785 120 Iyer, L.M. et al. (2004) Evolutionary history and higher order classification of AAA+
786 ATPases. *J Struct Biol* 146, 11–31
- 787 121 Leipe, D.D. et al. (2000) The bacterial replicative helicase DnaB evolved from a
788 RecA duplication. *Genome Research* 10, 5–16
- 789 122 Leipe, D.D. et al. (1999) Did DNA replication evolve twice independently? *Nucleic
790 Acids Res* 27, 3389–3401
- 791 123 Leipe, D.D. et al. (2003) Evolution and Classification of P-loop Kinases and Related
792 Proteins. *J Mol Biol* 333, 781–815

- 793 124 Kowalski, D. and Eddy, M.J. (1989) The DNA unwinding element: a novel, cis-
794 acting component that facilitates opening of the *Escherichia coli* replication origin. *The*
795 *EMBO journal* 8, 4335–4344
- 796 125 Richardson, T.T. et al. (2016) The bacterial DnaA-trio replication origin element
797 specifies ssDNA initiator binding. *Nature* 534, 412–416
- 798 126 Spinks, R.R. et al. (2021) Single-Molecule Insights Into the Dynamics of Replicative
799 Helicases. *Frontiers Mol Biosci* 8, 741718
- 800 127 Lo, C.-Y. and Gao, Y. (2021) DNA Helicase-Polymerase Coupling in Bacteriophage
801 DNA Replication. *Viruses* 13, 1739
- 802 128 Li, H. et al. (2020) Anatomy of a twin DNA replication factory. *Biochem Soc T* 48,
803 2769–2778
- 804 129 Yao, N.Y. and O'Donnell, M.E. (2020) The DNA Replication Machine: Structure and
805 Dynamic Function. *Subcell Biochem* 96, 233–258
- 806 130 Rousseau, F. et al. (2012) Implications of 3D domain swapping for protein folding,
807 misfolding and function. *Adv Exp Med Biol* 747, 137–152
- 808 131 Rousseau, F. et al. (2003) The unfolding story of three-dimensional domain
809 swapping. *Structure* 11, 243–251
- 810 132 Newcomer, M.E. (2002) Protein folding and three-dimensional domain swapping: a
811 strained relationship? *Curr Opin Struc Biol* 12, 48–53
- 812 133 Bennett, M.J. et al. (1995) 3D domain swapping: a mechanism for oligomer
813 assembly. *Protein Sci* 4, 2455–2468
- 814 134 Schlunegger, M.P. et al. (1997) Oligomer formation by 3D domain swapping: a
815 model for protein assembly and misassembly. *Adv Protein Chem* 50, 61–122
- 816 135 Hakansson, M. and Linse, S. (2002) Protein reconstitution and 3D domain
817 swapping. *Curr Protein Pept Sc* 3, 629–642
- 818 136 Aravind, L. et al. (2004) A novel family of P-loop NTPases with an unusual phyletic
819 distribution and transmembrane segments inserted within the NTPase domain. *Genome*
820 *Biol* 5, R30
- 821 137 Leipe, D.D. et al. (2002) Classification and evolution of P-loop GTPases and related
822 ATPases11Edited by J. Thornton. *J Mol Biol* 317, 41–72
- 823 138 Longo, L.M. et al. (2020) On the emergence of P-Loop NTPase and Rossmann
824 enzymes from a Beta-Alpha-Beta ancestral fragment. *Elife* 9, e64415

- 825 139 Walker, J.E. et al. (1982) Distantly related sequences in the alpha- and beta-
826 subunits of ATP synthase, myosin, kinases and other ATP-requiring enzymes and a
827 common nucleotide binding fold. *Embo J* 1, 945–951
- 828 140 Saraste, M. et al. (1990) The P-loop — a common motif in ATP- and GTP-binding
829 proteins. *Trends Biochem Sci* 15, 430–434
- 830 141 Neuwald, A.F. et al. (1999) AAA+: A class of chaperone-like ATPases associated
831 with the assembly, operation, and disassembly of protein complexes. *Genome*
832 *Research* 9, 27–43
- 833 142 Jez, J.M. (2017) Revisiting protein structure, function, and evolution in the genomic
834 era. *J Invertebr Pathol* 142, 11–15
- 835 143 Theobald, D.L. and Wuttke, D.S. (2005) Divergent Evolution Within Protein
836 Superfolds Inferred from Profile-based Phylogenetics. *J Mol Biol* 354, 722–737
- 837 144 Stebbins, C.E. and Galán, J.E. (2001) Structural mimicry in bacterial virulence.
838 *Nature* 412, 701–705
- 839

394 **Highlights**

395 • The initiation of DNA replication is a tightly regulated process in all cellular
396 domains of life and involves regulated recruitment and assembly of essential factors,
397 including the replicative hexameric helicase complex, to replication origins.

398 • A crucial step during the replication initiation phase of DNA replication is loading
399 of hexameric, ring-shaped replicative helicases onto DNA.

400 • In bacteria, the DnaB family of replicative helicases comprise six identical
401 subunits which collectively create a central chamber to bind one of the ssDNA strands of
402 dsDNA. The translocation of DnaB on ssDNA ahead of the DNA polymerase in the
403 replisome separates the two strands to provide substrates for DNA synthesis.

404 • Recent structure determinations of two bacterial helicase loaders bound to the
405 same DnaB helicase offers an opportunity to extract fundamental principles associated
406 with DnaB opening and loading onto ssDNA.

407 • *E. coli* DnaC and bacteriophage λ P evolved independently to converge, through
408 molecular mimicry, on a common helicase opening mechanism.

409

410 **Outstanding Questions**

- 411 • Is origin melting an emergent property that completely occurs completely through
412 formation of the initiator•DNA complex?
- 413 • Does the DnaB bacterial replicative helicase also contribute to opening of the
414 replication bubble as seen with the eukaryotic replicative helicase [117]?
- 415 • What mechanisms ensure the loading of two, and only two, helicases per initiation
416 event?
- 417 • What mediates helicase loading in opposite orientations?
- 418 • What mechanisms promote the eviction of the helicase loaders?
- 419 • What, if any, of the mechanisms implemented by the DciA and DopE loader are
420 in common with those used by DnaC or λ P?
- 421

294 **Glossary**295 **Replication origin** – DNA sequence on a chromosome where DNA synthesis will begin.296 In bacteria, replication origins are up to hundreds of base-pairs in length and
297 contain segments that are bound in a duplex state by the DnaA initiator protein, as
298 well as segments that are melted (e.g., the DNA unwinding element (DUE) [124]
299 DnaA trios [125] by the initiator [13,20,28,29].300 **DnaA** – The bacterial replication initiator protein (*E. coli*: 467 amino acids) is comprised
301 of four structural domains. Domain I harbors a K homology (KH) domain, domain
302 II is a linker element, domain III encompasses the AAA+ ATPase functionality, and
303 domain IV encodes a double-stranded helix-turn-helix DNA binding domain
304 [10,12,30–32].305 **DnaB** – The replicative helicase found in Gram-negative bacterial (*E. coli*: 471 amino
306 acids) [4,12–14,50]. It is related to the DnaC helicase found in Gram-positive
307 organisms.308 **DnaC** – The replicative helicase loader found in certain Gram-negative bacteria (*E. coli*:
309 245 amino acids) [4,10,16,51–55]. This analog of this protein in Gram-positive
310 species is Dnal.311 **Phage λ O** – The replication initiator protein (299 amino acids) used by phage λ . λ O
312 specifically recognizes a series of dsDNA binding sites in the phage λ replication
313 origin [41–49].314 **Phage λ P** – The helicase loader protein (233 amino acids) used by phage λ to assemble
315 the DnaB helicase at the phage λ replication origin [43,45–48,56–59].316 **Replisome** – A large (1-2 MDa) multi-protein complex that mediates synthesis of both
317 strands (leading and lagging) of DNA. The replisome consists of 2-3 DNA
318 polymerases, the replicative helicase, the sliding clamp, and the sliding clamp
319 loader. Other proteins such as single-stranded DNA binding protein, gyrase,
320 RNase H, and DNA ligase interface with the replisome to support leading and
321 lagging strand synthesis [126–129].322 **Domain-swapped oligomer** – An unusual architectural feature of some oligomeric
323 protein ensembles wherein members of the assembly exchange a structural
324 domain in a manner akin to a handshake between two persons. Swapping involves
325 replacement of intra-monomer interactions between two sub-domains with nearly
326 identical inter-monomer contacts. Such an oligomer becomes structurally
327 intertwined because of the domain swapping [130–135].328 **Phosphate - Loop (P-loop) NTPases** – Together with the Rossmann fold family, P-loop
329 NTPases encompass two major families of nucleotide handling proteins; proteins
330 in this family couple the energy of nucleotide binding and hydrolysis to some
331 chemical or mechanical transformation [123,136–138]. In concert with the crucial
332 role played by ATP and other nucleotides in biology, P-loop NTPases family
333 represent between 10 - 20% of all proteins in genomes in all cellular domains of
334 life [137]. Members of this family share a conserved overall fold consisting of a
335 four- or five-stranded beta-sheet sandwiched between two layers of alpha-helices;

336 this domain also exhibits two conserved amino acid sequence motifs termed the
337 Walker A and Walker B (so named after John Walker, who first observed them in
338 the F1 ATPases [139,140]). The Walker A sequence motif, which is the P-loop
339 itself, is a glycine-rich loop terminated by a threonine or serine (GxxGxGK[T/S],
340 where x = any residue); the backbone of this element makes a close approach to
341 the β and γ phosphates of ATP, while the lysine and the threonine/serine contact
342 the β phosphate and an associated Mg^{2+} ion, respectively. The Walker B sequence
343 motif is a run of hydrophobic residues terminated by an aspartate residue (hhhhD;
344 h = hydrophobic residue); the Walker B aspartate residue contributes to positioning
345 the Mg ion and its associated water molecules. Sequence and structural analyses
346 of P-loop NTPase family proteins highlight two major sub-divisions: the kinase –
347 GTPase (KG) and the ASCE (additional strand catalytic glutamate) families. The
348 ASCE grouping is further sub-classified into the RecA/F₁-F₀ ATPases, AAA+
349 ATPases, ABC ATPases, nucleic acid helicases, PilT/FtsK ATPases, apoptotic
350 NTPases, and the NACHT ATPases [123,137].

351 **RecA-like ATPases** – A sub-class of the ASCE sub-division of the P-loop NTPases.
352 Members of this family adopt oligomeric configurations, and include the RecA
353 recombinase, the DnaB replicative helicase, the F₁ sub-structure of ATP synthase,
354 and the Rho helicase, [114,123,136,137]. All the elements found in the ASCE sub-
355 class are seen in the RecA-like ATPases, as well as some additional structural
356 elements. Amongst these is an arginine finger that enables stimulation of ATP
357 hydrolysis *in trans* of nucleotide bound primarily by a neighboring subunit of the
358 oligomer.

359 **AAA+ ATPases** – A sub-class of the ASCE sub-division of the P-loop NTPases. AAA+
360 (ATPases Associated with various Activities) are a large family of oligomeric, often
361 ring-shaped, motors and switches with crucial functions in DNA replication,
362 transcription, chaperones, proteases, and beyond [89,100,141]. This family of
363 ATPases folds into a two-domain structure, one of which corresponds to the ASCE
364 core domain (the second is a small helical domain). Residues and motifs
365 conserved in this sub-class surround the general volume occupied by nucleotide.
366 ATP binding sites are formed at subunit interfaces. Most of the contacts to bound
367 nucleotide arise from one subunit at the interface, but the binding site is only
368 completed by participation of residues (e.g., arginine finger) from a neighboring
369 subunit.

370 **Convergent evolution** – a form of molecular evolution in which unrelated molecules
371 independently evolve similar shapes or properties that reflect intrinsic structural or
372 chemical constraints. Convergent evolution in the active sites of proteins has been
373 documented in several enzymes [108]. It is axiomatic that a common ancestor is
374 not present with examples of convergent evolution; by contrast, a common
375 ancestor is an essential feature of divergent evolution [142,143].

376 **Molecular mimicry** – Close structural resemblance between two molecular entities.
377 Mimicry can arise from divergent or convergent evolution [144].

[Click here to view linked References](#)

379 **Text Box:**

380 **Loading Bacterial Hexameric Replicative Helicases onto DNA**

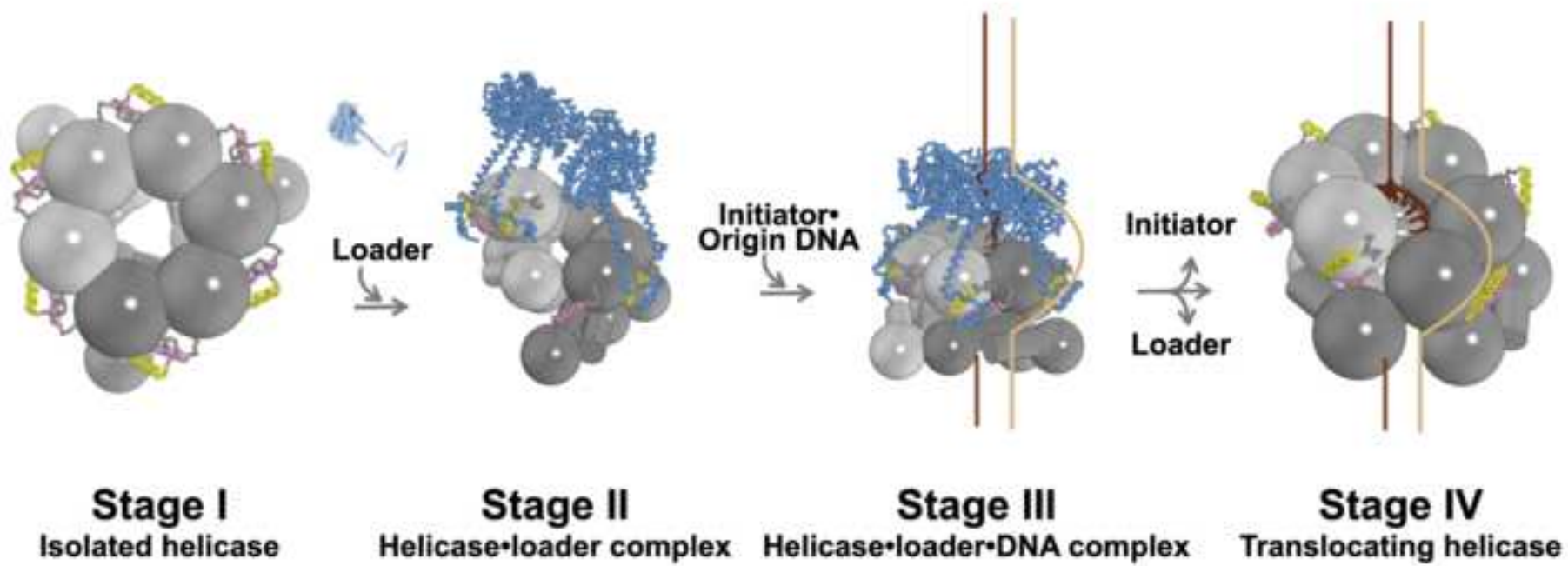
381 **Ring-breakers** – Loading factors that physically open hexameric helicase rings. *E. coli*
382 DnaC and λ P are two examples of replicative helicase loaders that bind to a pre-
383 formed closed DnaB ring and breach one its six subunit interfaces to enable
384 ssDNA to enter an internal chamber.

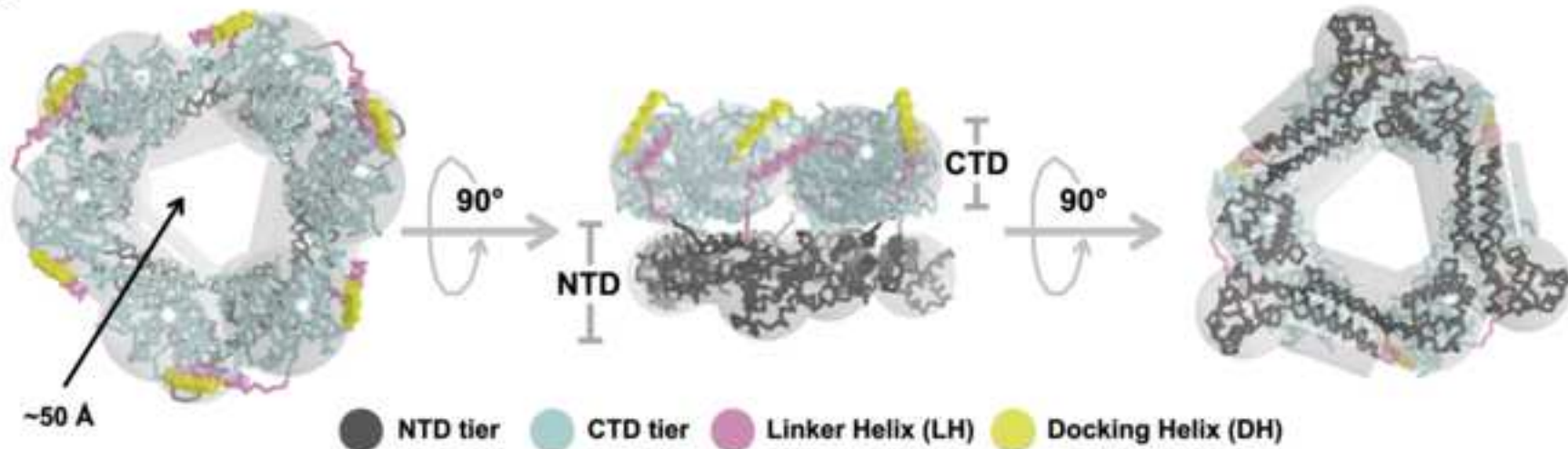
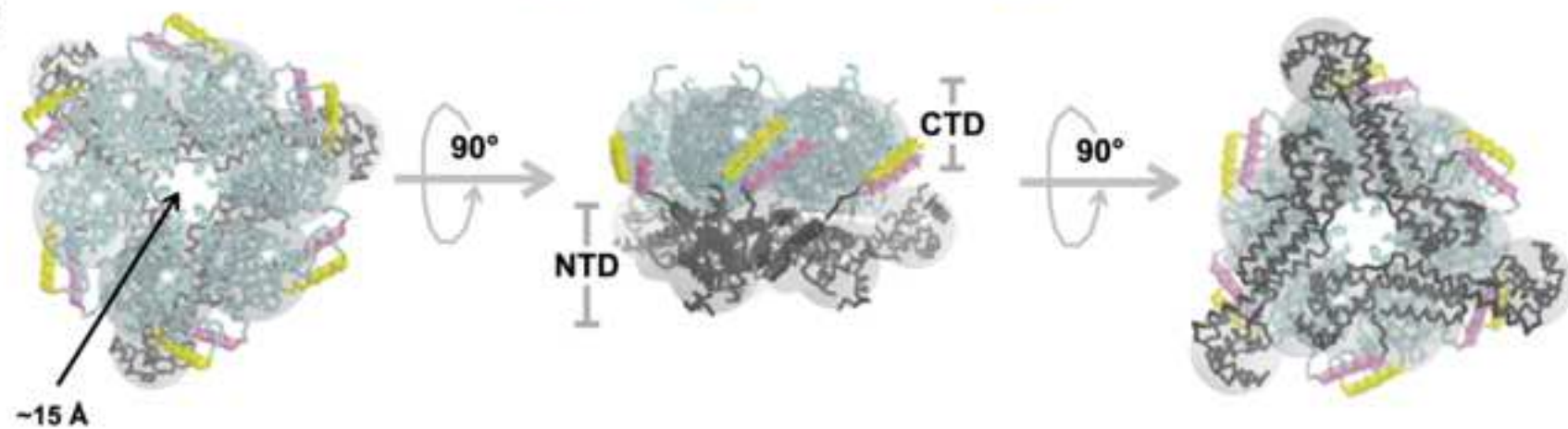
385 **Ring-makers** – Loading factors that assemble helicase monomers into hexameric rings.
386 *B. subtilis* Dnal is a bacterial helicase loader that is reported to operate in this
387 manner.

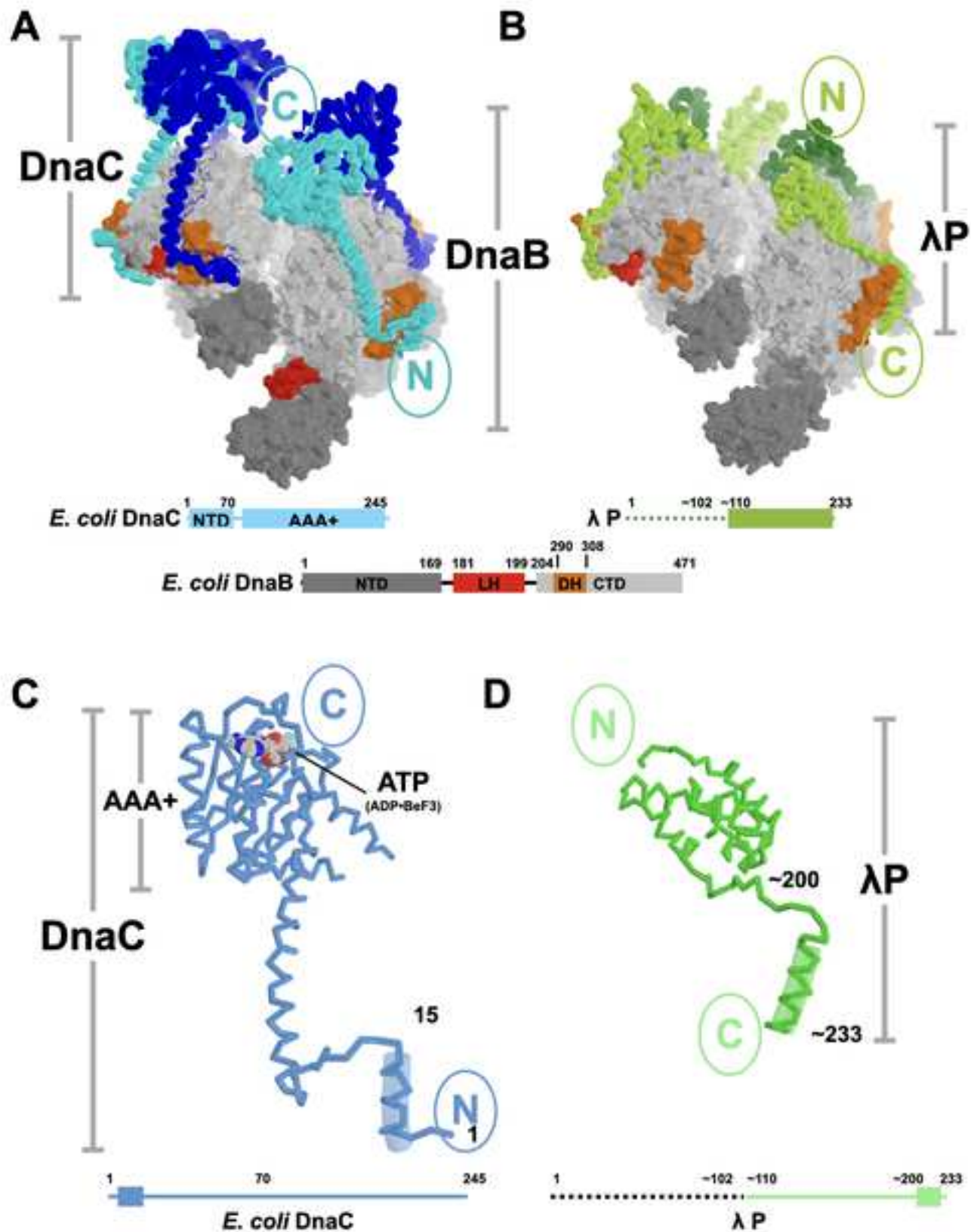
388 Mechanisms of bacterial helicase loaders in the DciA/DopE families remain to be
389 established. Distinct loading mechanisms with other hexameric helicases have
390 also been described, including self-regulated ring closure for the transcription
391 terminator Rho ATPase and chaperoned ring-closure for the MCM2-7 complex in
392 eukaryotic DNA replication (reviewed in [114]).

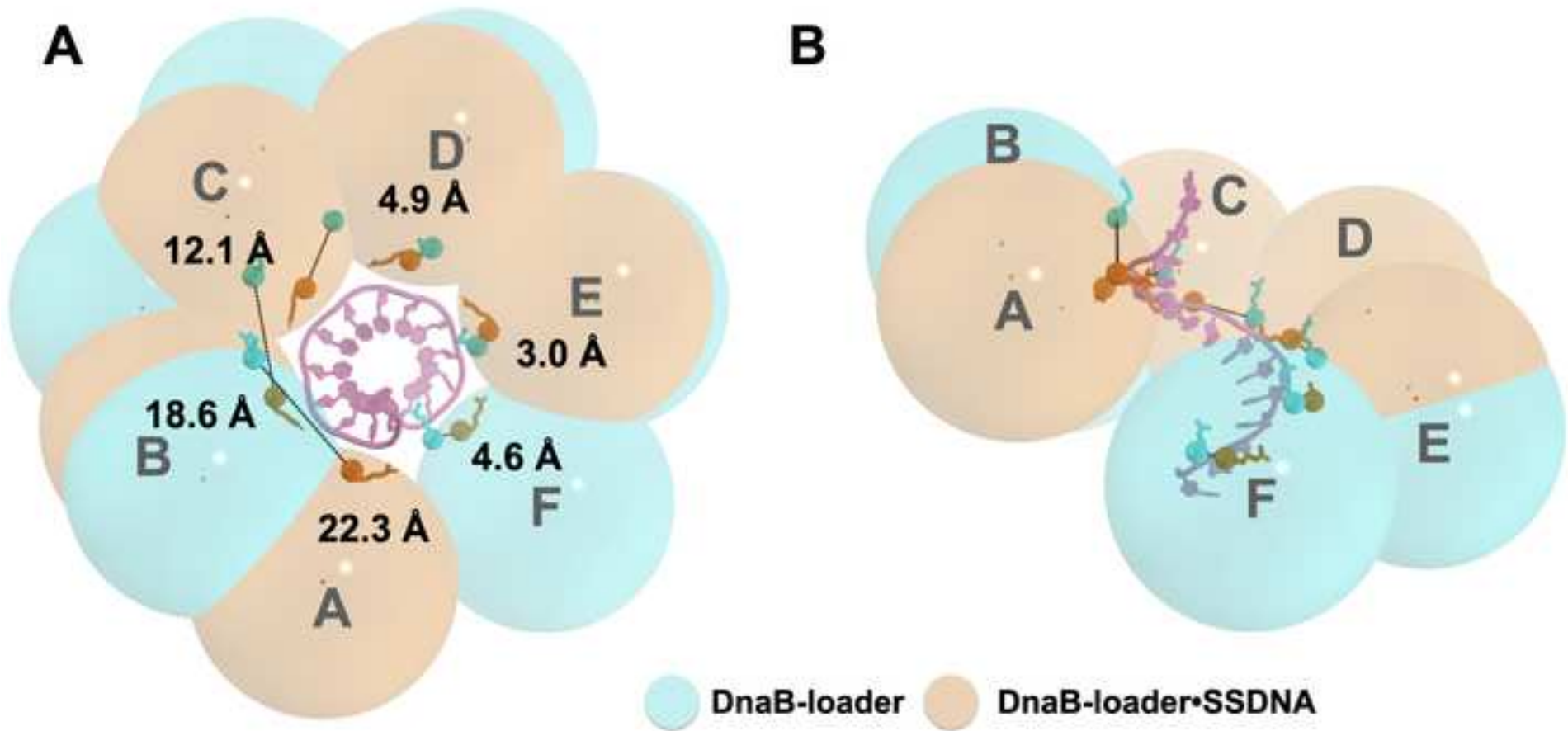
393

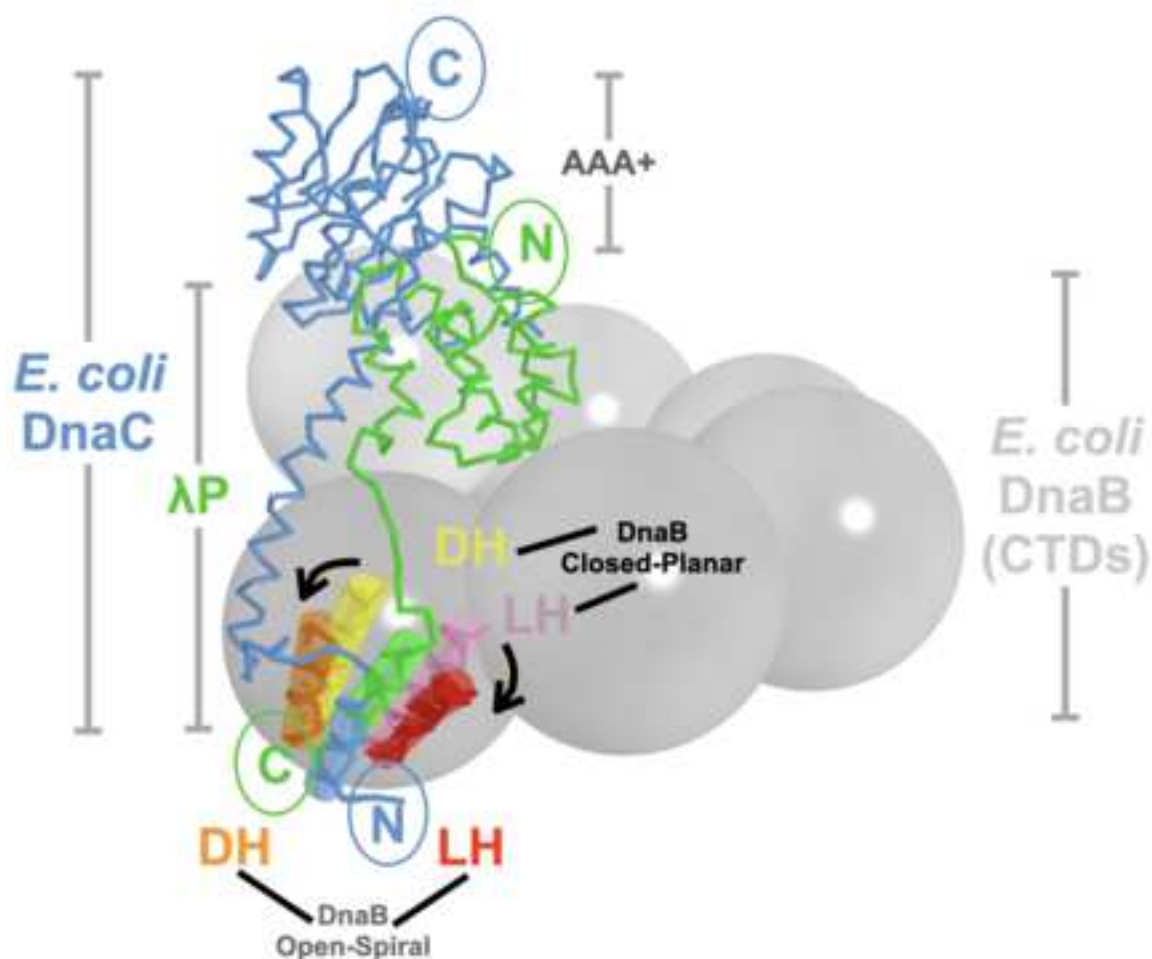
	<i>E. coli</i>	phage λ	<i>V. cholerae</i>
origin DNA	OriC	Oriλ	OriC-I/II
initiator	DnaA	O	DnaA/RctB
helicase	DnaB	DnaB	DnaB
loader	DnaC	P	DciA



A**B**







1 Convergent Evolution in Two Bacterial Replicative Helicase Loaders

2

3 Jillian Chase^{1,2}, James Berger^{3#}, and David Jeruzalmi^{1,2,4,5#}4 ¹Department of Chemistry and Biochemistry, City College of New York, New York,
5 NY 10031, USA;6 ³Department of Biophysics and Biophysical Chemistry, Johns Hopkins School of
7 Medicine, Baltimore, MD 212058 Ph.D. Programs in Biochemistry², Biology⁴, and Chemistry⁵, The Graduate Center
9 of the City University of New York, New York, NY 10016, USA;10 #Correspondence: dj@ccny.cuny.edu (Jeruzalmi, D) or jmberger@jhmi.edu
11 (Berger, J)

12 **Abstract (120 words)**

13 Dedicated loader proteins play essential roles in bacterial DNA replication by
14 opening ring-shaped DnaB-family helicases and chaperoning ssDNA into a central motor
15 chamber as a prelude to DNA unwinding. Although unrelated in sequence, the *E. coli*
16 DnaC and bacteriophage λ P loaders feature a similar overall architecture: a globular
17 domain linked to an extended lasso/grappling hook element, located at their amino and
18 carboxy termini, respectively. Both loaders remodel a closed DnaB ring into nearly
19 identical right-handed open conformations. The sole element shared by the loaders is a
20 single alpha helix, which binds to the same site on the helicase. Physical features of the
21 loaders establish that DnaC and λ P evolved independently to converge, through
22 molecular mimicry, on a common helicase opening mechanism.

23

24 **Keywords**

25 DnaB, DnaC, λ P, DciA, DNA Replication, helicase loading, convergent evolution,
26 molecular mimicry.

27

28 **Introduction (~3100 words)**

29 **Specialized Factors Load the DnaB Bacterial Replicative Helicase onto the**
30 **Replication Origin**

31 The regulated loading of ring-shaped hexameric helicases onto chromosomal
32 origins is an essential feature of DNA replication in all cellular domains of life [1–3].
33 Helicase deposition requires specialized factors known as helicase loaders, which
34 operate during the initiation of DNA replication [4–8]. In bacteria, several helicase loaders
35 have been studied, including *Escherichia coli* (*E. coli*) DnaC [4], bacteriophage λ P,
36 *Bacillus subtilis* (*B. subtilis*) DnaI [5], and DciA/DopE, a recently described class of
37 proteins which appear in bacteria that lack orthologs of DnaC or DnaI [6,7,9]. Helicase
38 loading is also critical to assembly of eukaryal and archaeal **replisomes** [1,2,8].

39 The assembly of the bacterial replicative helicase (**Figure 1**), which is known as
40 DnaB in most bacteria or DnaC in *B. subtilis* (henceforth called DnaB), onto origin DNA
41 occurs during the initiation phase of DNA replication [8,10–14]. Our view of replication
42 initiation in bacteria is informed by studies with primary and secondary chromosomes of
43 bacteria, plasmids, and phages [15–27], and have implied the involvement of four classes
44 of factors (**Table 1**): 1) a DNA sequence called a replication origin, where DNA synthesis
45 will begin [13,20,28,29], 2) a replication initiator protein (*E. coli*: DnaA [10,12,30–32], *V.*
46 *cholerae*: DnaA, RctB [18,21,23,25,33–37], plasmids: RepE, Pi, TrfA [38–40], phage
47 lambda (λ): O [41–49]), 3) a DnaB-family replicative helicase [4,12–14,50], and, finally, 4)
48 a helicase loader (*E. coli*: DnaC [4,10,16,51–55], phage λ: P [43,45–48,56–59], *V.*
49 *cholerae*: DciA [6,9]). The multi-step process for initiating DNA replication begins with the
50 recognition and binding of multiple copies of the initiator protein to dsDNA sites at the

51 replication origin; once bound, initiator proteins associate into a complex protein-DNA
52 ensemble [4,10,12,19,31,60,61]. One of the outputs of the initiation phase of DNA
53 replication is the melting of an A-T rich segment of the replication origin termed the DNA
54 unwinding element (DUE) by the DnaA or the λ O initiator proteins [13,30,31], an event
55 that provides single DNA strands (ssDNA) as substrates for DnaB loading. DnaB
56 hexamers assemble into two-tiered rings formed by the amino (NTD) and carboxy-
57 terminal domains (CTD) of the helicase; a so-termed 'linker helix' element (LH) connects
58 these domains and packs against another alpha helix, termed the docking helix (DH), of
59 a neighboring DnaB subunit to give rise to a **domain-swapped oligomer** [62–64] (Figure
60 **2**). The two DnaB tiers circumscribe an internal chamber into which one of the ssDNA
61 strands from the replication origin will be loaded. One layer is formed out of six NTDs,
62 which assemble into two different 'trimer-of-dimers' configurations that display pseudo-
63 three-fold symmetry. These arrangements arise from alternative packing orientations for
64 NTD dimers, which create several types of subunit interfaces of likely varying stability
65 [62,65]. The CTD tier assembles out of six C-terminal domains (CTD) of DnaB, each of
66 which harbors a **RecA-like ATPase domain**. In contrast to the NTD, the CTD layer
67 exhibits a pseudo-six-fold arrangement, with a single type of interface.

68 Helicase loading onto ssDNA can be conceptually divided into four stages (Figure
69 **1**). During assembly, DnaB transitions between three conformations: closed planar, open
70 right-handed spiral, and closed right-handed spiral [62–68]. In addition, the NTD and
71 CTD layers of each of these conformers are found in one of two arrangements: dilated or
72 constricted (**Figures 2A-2B**); these conformers differ on inter-protomer contacts. The
73 isolated hexameric helicase, in both dilated and constricted closed-planar configurations,

74 populates Stage I. Formation of the helicase•helicase loader complex leads to Stage II,
75 while engagement of the helicase•loader complex with origin-derived ssDNA•initiator
76 (DnaA or λ O) populates Stage III. The ATPase and ssDNA translocation activities of the
77 helicase are suppressed during these latter two stages [56,58,69–71], with **the**
78 **DnaA/replication origin complex** also playing a role in loading or positioning the
79 **helicase/loader complex** using direct contacts between DnaA and DnaB [69–71] (the
80 **involvement of contacts between other bacterial replication initiators and DnaB** remains
81 **to be clarified**). Recently, cryogenic electron microscopy (cryo-EM) analyses of two
82 distinct bacterial helicase•loader complexes (*E. coli* DnaB•DnaC and *E. coli* DnaB• λ P,
83 **Figure 1: Stages II-III, and Figure 3**) have shown that the helicase adopts an open right-
84 handed spiral configuration, promoted, and stabilized by interactions with the helicase
85 loaders [65,68]. The transition to Stage IV is accompanied by eviction of the loader and
86 initiator from the complex on DNA, which relieves inhibition of DnaB's activities. Notably,
87 in Stage III, the configuration of the DnaB-bound loader is nearly identical to the closed
88 spiral form seen in the loader-free helicase of Stage IV [65,67].

89 Helicase loading in bacteria occurs by one of at least two reported mechanisms
90 [72], termed: a) ring breaking, where DnaB hexamers are physically opened [73], and b)
91 ring making, in which hexamers are assembled [5]. It is now clear that both *E. coli* DnaC
92 and phage λ P are ring breakers: each loader binds to and delivers a pre-formed helicase
93 hexamer to its cognate origin [4,43,45–47,56,58,74]. DnaC and λ P are similar in that
94 both are essential for their respective organisms and both bind to ssDNA [56,58,75–77].
95 λ P also can displace DnaC from *E. coli* DnaB, implying that their respective binding sites
96 overlap [58,74]. These congruencies might imply a common ancestry; however, DnaC

97 and λ P are unrelated in sequence and enzymatic function (e.g., DnaC is a known ATPase
98 [10,53,75–77], whereas λ P is not [78]). Moreover, although each loading system requires
99 ejection of the loader from the DNA complex for DnaB to transition to the translocation-
100 competent form, eviction occurs by distinct mechanisms. For DnaC, nucleotide dynamics
101 in its **AAA+ ATPase domain**, along with RNA synthesis by the DnaG primase, are
102 significant features in eviction [10,52,53,76,77,79]. By contrast, removal of λ P requires
103 the host DnaK/DnaJ/GrpE chaperone machinery [31–34]. **Helicase loading is also a**
104 **feature during restart of DNA replication after it has prematurely been halted in response**
105 **to DNA damage and involves a distinct set of proteins (PriA, PriB, PriC, and DnaT); the**
106 **reader is referred to the literature for a more complete treatment of helicase loading during**
107 **replication restart [80–82].**

108 Here, we compare recent structures of two bacterial helicase loaders: *E. coli* DnaC
109 [65] and phage λ P [68] bound to the same *E. coli* DnaB helicase (**Figure 3**). This
110 comparison provides an opportunity to understand the mechanisms of the two loaders
111 and to extract central principles associated with DnaB opening and loading onto ssDNA.
112 A recent crystal structure of the interaction domains of DnaB and DnaC [83] comports
113 with the EM analyses of the complete complexes. A new study of DciA•DnaB interactions
114 also points to some conserved elements of helicase opening in this system as well [9].
115 **Further study will be required to establish the mechanistic relationships, if any, between**
116 **the DciA and *B. subtilis* DnaI/DnaB/DnaD loaders [5,84,85] and the better understood *E.***
117 ***coli* DnaC [65] and λ P [68] systems.**

118

119 **Though unrelated by sequence and fold, *E. coli* DnaC and λ P exhibit analogous**
120 **global architectures**

121 Inspection of the *E. coli* DnaB•DnaC (BC) and the *E. coli* DnaB•phage λ P (BP)
122 complexes shows that the two loaders engage the carboxy-terminal (CTD) ATPase
123 surface of DnaB to form a three-layered ensemble [65,68,83]. One layer corresponds to
124 an oligomeric form of the helicase loader (hexameric for DnaC and pentameric for λ P),
125 while the second and third correspond to the NTD and CTD tiers of DnaB (**Figures 3A-**
126 **B**). **Although six copies of DnaC are present in the *E. coli* BC complex and five λ P**
127 **protomers are found in the BP assembly, the stoichiometries seen in the cryo-EM**
128 **structures do not necessarily preclude the possibility that complexes with fewer copies of**
129 **the loader might be active in supporting helicase loading.** Significantly, each loader
130 adopts a distinct and unrelated structure, yet the monomers of both exhibit a similar
131 overall architecture: a globular domain fused to an extended segment that forms a
132 lasso/grappling hook element (**Figures 3C-D**).

133 The globular domain of DnaC consists of an AAA+ ATPase module that is fused
134 to a ~75 residue N-terminal segment (**Figure 3C**)[65,83]. The amino-terminal segment
135 of DnaC consists of a long α-helix that extends along the CTD of a DnaB protomer and
136 initiates from a helix-loop-helix element that packs against the LH linker helix from one
137 DnaB subunit and the DH docking helix from another. Notably, the N-terminal segment
138 provides the only contacts between DnaC and the DnaB helicase. The six copies of the
139 globular DnaC AAA+ domain assemble into an open spiral like that seen in related
140 ATPases such as DnaA and archaeal/eukaryal MCM helicases [86–92]. In the absence
141 of ssDNA, five of the six nucleotide-binding sites in DnaC are populated with an ATP

142 analog (ADP•BeF₃), whereas the sixth (which sits at the gap in the DnaC spiral) engages
143 ADP, likely because its catalytic center lacks important functional contacts from a
144 neighboring protomer. Rationalizing this arrangement of nucleotides is the prior finding
145 that the ATP form of DnaC suppresses DnaB's helicase activity and as it stabilizes the
146 ssDNA complex [52].

147 For the λ P loader, only the C-terminal ~125 residues were resolved in EM density
148 maps [68]. This region consists of an α-helical globular domain fused to an extended
149 segment of ~45 residues (Figure 3D). The λ P extension forms a sub-structure
150 analogous to, but distinct from, that seen in DnaC [65,83], terminating in a single α-helix
151 that packs against the LH and DH elements of two adjacent subunits of DnaB. Both the
152 globular domain and the grappling hook/lasso segment of λ P contact two consecutive
153 subunits of the DnaB hexamer. These interactions are repeated in the five copies of λ P
154 in the BP complex to create an open helical arrangement of loaders; the breached
155 interface of the DnaB hexamer precludes binding of a sixth copy of λ P. The low resolution
156 (4.1 Å) of the BP EM maps in the region of the loader limits analysis of interfaces between
157 λ P protomers; nevertheless, an extensive interface between the five λ P protomers does
158 not appear to form.

159

160 ***E. coli* DnaC and phage λP reconfigure DnaB into an open right-handed spiral**

161 Despite their evolutionarily distinct structures and contacts with DnaB, both DnaC
162 and λ P reconfigure the helicase into highly similar, open-spiral configurations (root mean
163 square deviation (RMSD) of ~2.2 Å, calculated from 2611 C_α positions that span the

164 DnaB hexamer) [65,68]. The DnaB NTDs also both adopt a constricted configuration,
165 albeit with a spiral (as opposed to planar) shape that bears a split between one of the
166 subunit interfaces. The similarity between DnaB in the two loader complexes is also
167 evident from the average helical pitch and twist values of the open spirals in both the NTD
168 (~2.8 Å and 60.0° for BC vs. ~2.6 Å and 59.9° for BP) and CTD layers (~19.3 Å and
169 ~55.3° for BC vs. ~16 Å and ~56° for BP). Changes induced by each loader rupture one
170 of the DnaB subunit interfaces at both the NTD and CTD layers to create openings (15-
171 20 Å) of sufficient size to allow ssDNA access to the internal chamber.

172 Changes to the helical pitch and twist of the DnaB hexamer within each loader
173 complex combine to alter the configuration of the ssDNA-binding site in the helicase.
174 Superposition of DnaB from each loader complex reveals significant changes in the
175 position of DNA binding residues in comparison to that when DnaB is bound to ssDNA
176 (**Figure 4**) [65]. When bound to ssDNA and the loader, the CTD of each DnaB protomer
177 projects three residues (*E. coli*: R403, E404, G406) on a DNA binding loop into the
178 helicase pore to contact ssDNA. In the loader-only complexes, reconfiguration of the
179 CTD layer shifts the positions of the alpha-carbons of these residues by ~10-30 Å (in BC)
180 or ~5-20 Å (in BP).

181 The disposition and nucleotide occupancy of the six RecA-type ATPase sites in
182 DnaB are also altered in the complexes with DnaC and λ P [65,68]. ATPase activity by
183 DnaB relies on ‘composite’ nucleotide binding sites, wherein residues from two adjacent
184 subunits contribute to a single catalytic center [63,64,67,93]. In both helicase•loader
185 complexes, five of the six ATPase sites in DnaB are occupied by ADP, while the sixth,
186 which sits at the breach in the CTD ring, is vacant; when bound to just ssDNA, this

187 constellation of sites are filled with a nucleoside triphosphate analog (ADP•BeF₃) instead.
188 The alterations in CTD orientation appear to have remodeled the five ADP-filled sites of
189 the loader-bound helicase into non-optimal catalytic configurations as well, although the
190 resolution of the structures prevents a more precise evaluation of these changes [65,68].

191

192 **Two distinct helicase loader complexes with a shared function**

193 The BC and BP complexes reveal how the evolutionarily distinct structural
194 elements of DnaC and λ P converged on a common helicase-opening strategy [65,68].
195 In both loader complexes, the lasso/grappling hook segments of DnaC and λ P provide
196 key contacts to opening the DnaB helicase (**Figure 5**). Superposition of the two
197 complexes on a DnaB monomer reveals that the only segment in common between the
198 two loaders is a single α helix at the extreme amino-terminus of DnaC, or the carboxy-
199 terminus of λ P. In both complexes, this helix disrupts interactions between the LH linker
200 helix of one DnaB protomer and the DH docking helix on an adjacent subunit; each DnaB
201 protomer undergoes this interaction save for the one at the breach in the spiral. Insertion
202 of the loader α helix between the DnaB LH and DH elements reconfigures the CTD, and
203 concomitantly the NTD, tiers, from the closed planar to the open spiral form to allow
204 ssDNA to access the internal chamber of DnaB. Notably, in the BC structure, the N-
205 terminal lasso/grappling hook element represents the sole point of contact between DnaC
206 and DnaB; indeed, the isolated region harbors significant capacity to promote helicase
207 loading [66].

208 It was surprising to find that the AAA+ ATPase domains of DnaC make no contact
209 with DnaB, and thus, play no direct role in helicase opening (**Figure 3A**)[65]. By
210 comparison, the AAA+ ATPases of the evolutionarily related clamp loaders – which open
211 and chaperone the ring-shaped β and PCNA proteins onto DNA to aid polymerase
212 processivity – engage their client clamps directly [94–98]. For DnaC, the ATPase
213 elements appear to play a role in sensing the binding of ssDNA to the helicase and in
214 enhancing the efficiency of the DnaB-opening reaction [66]. **AAA+ ATPases are often**
215 **pre-formed oligomers** [99,100], unusually, in solution, DnaC is monomeric [54], however,
216 **six copies oligomerize on DnaB in a manner stabilized by ATP** [54,65]. Without ssDNA,
217 the nucleotide-binding sites of DnaC in the BC complex are filled with ATP and captured
218 in a configuration that is poised, but sub-optimal for catalysis. After sensing ssDNA, the
219 nucleotides sites on the DnaC oligomer are filled with ADP, as would be expected
220 following hydrolysis. ATP hydrolysis after ssDNA loading does not appear to allow DnaC
221 to dissociate from DnaB but may diminish stability of the DnaC oligomer. Biochemical
222 studies suggest that DnaG recruitment and primer synthesis are needed to promote loss
223 of DnaC from the complex [55,74,101].

224 In contrast to the modest interface between helicase and loader in the BC complex
225 [65,68], λ P forms an extensive interface with DnaB that encompasses both the globular
226 and lasso/grappling hook segments (**Figure 3B**). λ P is also a monomer in solution and
227 five copies assemble onto DnaB in the BP loader complex [68], however, few contacts
228 between loader subunits are seen. Inspection of the two loader complexes indicate that
229 the positioning of their C-terminal α helices between DnaB's LH and DH elements may
230 be sufficient for opening and that an extensive interface is dispensable for helicase

231 opening. This has been confirmed for DnaC [66], and we speculate that the extensive
232 interface between the DnaB and the globular domain of λ P may form because of
233 interacting with the opened helicase, rather than as its driver as previously proposed [68].
234 If so, then, what might be the functional role(s) for the extensive interface between λ P
235 and DnaB? Biochemical studies provide a potential explanation for the structural
236 dichotomy. It is known that λ P can displace DnaC from a preformed BC complex [58];
237 the extensive interface in the BP complex may aid displacement as part of a biological
238 strategy to appropriate the host replication machinery away from the bacterial
239 chromosome and toward the phage genome. Alternatively, the extensive interface in the
240 BP complex may serve as a functional analogue to the extensive AAA+ interaction
241 between DnaC globular domains in the BC complex. Regardless, in both the BC and BP
242 complexes, overall stability is achieved by oligomerization, but by distinct means [65,68].

243 Although they feature some global architectural parallels, neither the globular
244 domains of DnaC and λ P nor the extended lasso/grappling hook regions display any
245 similarity in sequence [65,68]. Underscoring the dissimilarity is the opposing chain
246 polarity of the grappling hook segments as they run across the surface of DnaB: DnaC
247 runs N-to-C whereas λ P runs C-to-N (**Figures 3C-3D and Figure 5**). The finding that a
248 single functionally significant α -helix in DnaC and λ P exhibits a divergent protein chain
249 direction confirms their lack of evolutionary kinship and instead reflects a form of
250 **molecular mimicry** that arose through **convergent evolution**. Molecular mimicry in
251 bacterial DNA replication initiation joins other examples from protein synthesis [102–104],
252 gene expression [105], apoptosis [106], host pathogen interactions [107–109], virally
253 encoded proteins[110], and immunity and autoimmunity [111].

254

255 **A recently described protein known as DciA serves as the primary helicase loader**
256 **in bacteria that lack DnaC/Dnal**

257 Outside of DnaC and λ P, Ferat and co-workers have reported that most bacteria
258 lack homologs of DnaC (or the unrelated Dnal loader) and that helicase loading in these
259 organisms instead appears to depend on a distinct protein called DciA [6] (**Table 1**). A
260 structure of DciA from *Vibrio cholerae* (VcDciA) shows that the protein is composed of an
261 ~110 aa N-terminal globular domain followed by a ~40 aa disordered C-terminal segment.
262 Interestingly, the fold of the DciA globular domain is related to the N-terminal domain of
263 the replication initiator, DnaA, as well as the C-terminal domain of the γ/τ /DnaX clamp
264 loader subunit and the FliK flagellar hook-length control protein. VcDciA appears to
265 stimulate the loading of the VcDnaB helicase onto DNA through a DciA₃:DnaB₆
266 intermediate; the LH-DH nexus that is targeted by DnaC and λ P has been suggested to
267 serve as an important point of contact in this complex as well [9]. It has been proposed
268 that VcDnaB may adopt an open spiral in solution and may harbor residues that specify
269 loader preference. Given the widespread nature of the DciA system, additional chapters
270 of the helicase loader story clearly remain to be written.

271

272 **Concluding Remarks**

273 In all cellular organisms, the regulated association of the replicative helicase with
274 replication origins sets the stage for the initiation of DNA replication [1–8] (**Table 1** and
275 **Figure 1**). However, significant differences are now evident in mechanisms by which

276 origin unwinding and helicase loading take place in bacteria as compared to archaea and
277 eukaryotes. In bacterial replication systems, the current model holds that the initiator
278 protein not only marks an origin for initiation, but also melts that origin, enabling the
279 replicative helicase•loader complex to load onto the resultant ssDNA [8,12,13,31,112].
280 By contrast, in archaea and eukaryotes, the helicase is loaded by an initiator complex
281 around duplex DNA, which is then subsequently melted by the helicase itself [113–118].
282 These distinct mechanisms are remarkable given that replication initiation machinery in
283 all three domains of life is predicated on a related AAA+ fold [8,13,86]. Why the two
284 approaches arose during evolution is unclear but may reflect an adaption to the two
285 different families of hexameric helicases – one based on a RecA ATPase fold, and
286 another based on a AAA+ ATPase domain [119–123] – that have been employed to
287 support replication in bacteria as compared to archaea and eukaryotes. Structural
288 analyses of two bacterial loaders bound to the *E. coli* DnaB helicase have for the first time
289 illuminated the rich detail and diversity of helicase-ring opening as well as DNA
290 association (**Figures 2, 3, 4 and Figure 5**). However, despite the insights gained from
291 these models, several fundamental questions about replication initiation and helicase
292 loading remain to be addressed (Outstanding Questions).

293

294 **Glossary**

- 295 **Replication origin** – DNA sequence on a chromosome where DNA synthesis will begin.
296 In bacteria, replication origins are up to hundreds of base-pairs in length and
297 contain segments that are bound in a duplex state by the DnaA initiator protein, as
298 well as segments that are melted (e.g., the DNA unwinding element (DUE) [124]
299 DnaA trios [125] by the initiator [13,20,28,29].
- 300 **DnaA** – The bacterial replication initiator protein (*E. coli*: 467 amino acids) is comprised
301 of four structural domains. Domain I harbors a K homology (KH) domain, domain
302 II is a linker element, domain III encompasses the AAA+ ATPase functionality, and
303 domain IV encodes a double-stranded helix-turn-helix DNA binding domain
304 [10,12,30–32].
- 305 **DnaB** – The replicative helicase found in Gram-negative bacterial (*E. coli*: 471 amino
306 acids) [4,12–14,50]. It is related to the DnaC helicase found in Gram-positive
307 organisms.
- 308 **DnaC** – The replicative helicase loader found in certain Gram-negative bacteria (*E. coli*:
309 245 amino acids) [4,10,16,51–55]. This analog of this protein in Gram-positive
310 species is Dnal.
- 311 **Phage λ O** – The replication initiator protein (299 amino acids) used by phage λ . λ O
312 specifically recognizes a series of dsDNA binding sites in the phage λ replication
313 origin [41–49].
- 314 **Phage λ P** – The helicase loader protein (233 amino acids) used by phage λ to assemble
315 the DnaB helicase at the phage λ replication origin [43,45–48,56–59].
- 316 **Replisome** – A large (1-2 MDa) multi-protein complex that mediates synthesis of both
317 strands (leading and lagging) of DNA. The replisome consists of 2-3 DNA
318 polymerases, the replicative helicase, the sliding clamp, and the sliding clamp
319 loader. Other proteins such as single-stranded DNA binding protein, gyrase,
320 RNase H, and DNA ligase interface with the replisome to support leading and
321 lagging strand synthesis [126–129].
- 322 **Domain-swapped oligomer** – An unusual architectural feature of some oligomeric
323 protein ensembles wherein members of the assembly exchange a structural
324 domain in a manner akin to a handshake between two persons. Swapping involves
325 replacement of intra-monomer interactions between two sub-domains with nearly
326 identical inter-monomer contacts. Such an oligomer becomes structurally
327 intertwined because of the domain swapping [130–135].
- 328 **Phosphate - Loop (P-loop) NTPases** – Together with the Rossman fold family, P-loop
329 NTPases encompass two major families of nucleotide handling proteins; proteins
330 in this family couple the energy of nucleotide binding and hydrolysis to some
331 chemical or mechanical transformation [123,136–138]. In concert with the crucial
332 role played by ATP and other nucleotides in biology, P-loop NTPases family
333 represent between 10 - 20% of all proteins in genomes in all cellular domains of
334 life [137]. Members of this family share a conserved overall fold consisting of a
335 four- or five-stranded beta-sheet sandwiched between two layers of alpha-helices;

336 this domain also exhibits two conserved amino acid sequence motifs termed the
337 Walker A and Walker B (so named after John Walker, who first observed them in
338 the F1 ATPases [139,140]). The Walker A sequence motif, which is the P-loop
339 itself, is a glycine-rich loop terminated by a threonine or serine (GxxGxGK[T/S],
340 where x = any residue); the backbone of this element makes a close approach to
341 the β and γ phosphates of ATP, while the lysine and the threonine/serine contact
342 the β phosphate and an associated Mg^{2+} ion, respectively. The Walker B sequence
343 motif is a run of hydrophobic residues terminated by an aspartate residue (hhhhD;
344 h = hydrophobic residue); the Walker B aspartate residue contributes to positioning
345 the Mg ion and its associated water molecules. Sequence and structural analyses
346 of P-loop NTPase family proteins highlight two major sub-divisions: the kinase –
347 GTPase (KG) and the ASCE (additional strand catalytic glutamate) families. The
348 ASCE grouping is further sub-classified into the RecA/F₁-F₀ ATPases, AAA+
349 ATPases, ABC ATPases, nucleic acid helicases, PilT/FtsK ATPases, apoptotic
350 NTPases, and the NACHT ATPases [123,137].

351 **RecA-like ATPases** – A sub-class of the ASCE sub-division of the P-loop NTPases.
352 Members of this family adopt oligomeric configurations, and include the RecA
353 recombinase, the DnaB replicative helicase, the F₁ sub-structure of ATP synthase,
354 and the Rho helicase, [114,123,136,137]. All the elements found in the ASCE sub-
355 class are seen in the RecA-like ATPases, as well as some additional structural
356 elements. Amongst these is an arginine finger that enables stimulation of ATP
357 hydrolysis *in trans* of nucleotide bound primarily by a neighboring subunit of the
358 oligomer.

359 **AAA+ ATPases** – A sub-class of the ASCE sub-division of the P-loop NTPases. AAA+
360 (ATPases Associated with various Activities) are a large family of oligomeric, often
361 ring-shaped, motors and switches with crucial functions in DNA replication,
362 transcription, chaperones, proteases, and beyond [89,100,141]. This family of
363 ATPases folds into a two-domain structure, one of which corresponds to the ASCE
364 core domain (the second is a small helical domain). Residues and motifs
365 conserved in this sub-class surround the general volume occupied by nucleotide.
366 ATP binding sites are formed at subunit interfaces. Most of the contacts to bound
367 nucleotide arise from one subunit at the interface, but the binding site is only
368 completed by participation of residues (e.g., arginine finger) from a neighboring
369 subunit.

370 **Convergent evolution** – a form of molecular evolution in which unrelated molecules
371 independently evolve similar shapes or properties that reflect intrinsic structural or
372 chemical constraints. Convergent evolution in the active sites of proteins has been
373 documented in several enzymes [108]. It is axiomatic that a common ancestor is
374 not present with examples of convergent evolution; by contrast, a common
375 ancestor is an essential feature of divergent evolution [142,143].

376 **Molecular mimicry** – Close structural resemblance between two molecular entities.
377 Mimicry can arise from divergent or convergent evolution [144].

379 **Text Box:**

380 **Loading Bacterial Hexameric Replicative Helicases onto DNA**

381 **Ring-breakers** – Loading factors that physically open hexameric helicase rings. *E. coli*
382 DnaC and λ P are two examples of replicative helicase loaders that bind to a pre-
383 formed closed DnaB ring and breach one its six subunit interfaces to enable
384 ssDNA to enter an internal chamber.

385 **Ring-makers** – Loading factors that assemble helicase monomers into hexameric rings.
386 *B. subtilis* Dnal is a bacterial helicase loader that is reported to operate in this
387 manner.

388 Mechanisms of bacterial helicase loaders in the DciA/DopE families remain to be
389 established. Distinct loading mechanisms with other hexameric helicases have
390 also been described, including self-regulated ring closure for the transcription
391 terminator Rho ATPase and chaperoned ring-closure for the MCM2-7 complex in
392 eukaryotic DNA replication (reviewed in [114]).

393

394 **Highlights**

395 • The initiation of DNA replication is a tightly regulated process in all cellular
396 domains of life and involves regulated recruitment and assembly of essential factors,
397 including the replicative hexameric helicase complex, to replication origins.

398 • A crucial step during the replication initiation phase of DNA replication is loading
399 of hexameric, ring-shaped replicative helicases onto DNA.

400 • In bacteria, the DnaB family of replicative helicases comprise six identical
401 subunits which collectively create a central chamber to bind one of the ssDNA strands of
402 dsDNA. The translocation of DnaB on ssDNA ahead of the DNA polymerase in the
403 replisome separates the two strands to provide substrates for DNA synthesis.

404 • Recent structure determinations of two bacterial helicase loaders bound to the
405 same DnaB helicase offers an opportunity to extract fundamental principles associated
406 with DnaB opening and loading onto ssDNA.

407 • *E. coli* DnaC and bacteriophage λ P evolved independently to converge, through
408 molecular mimicry, on a common helicase opening mechanism.

409

410 **Outstanding Questions**

411 • Is origin melting an emergent property that completely occurs completely through
412 formation of the initiator•DNA complex?

413 • Does the DnaB bacterial replicative helicase also contribute to opening of the
414 replication bubble as seen with the eukaryotic replicative helicase [117]?

415 • What mechanisms ensure the loading of two, and only two, helicases per initiation
416 event?

417 • What mediates helicase loading in opposite orientations?

418 • What mechanisms promote the eviction of the helicase loaders?

419 • What, if any, of the mechanisms implemented by the DciA and DopE loader are
420 in common with those used by DnaC or λ P?

421

422 **Acknowledgements**

423 This work was supported by the National Science Foundation (DJ: MCB 1818255),
424 the National Institutes of Health (DJ: R-01-GM084162 JMB: R37-071747), and the
425 Department of Education (JC: PA200A150068).

426

427

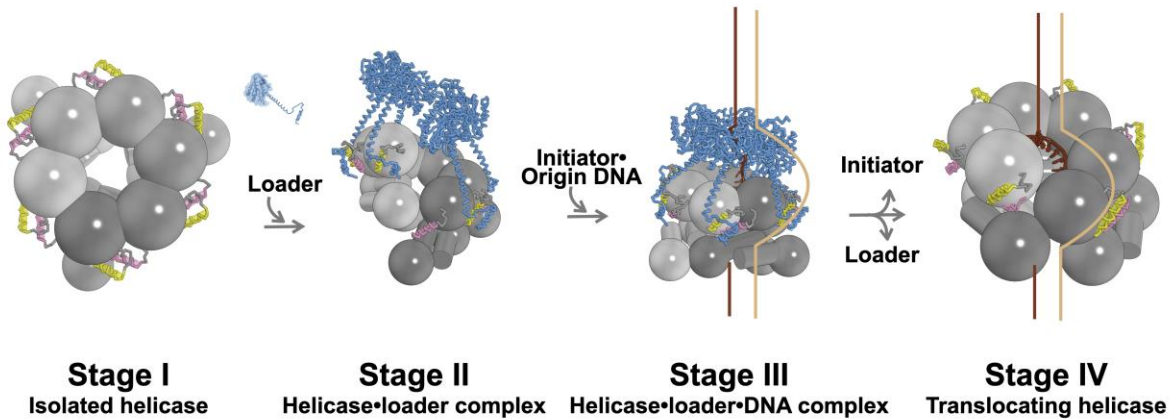
428 **Figure legends**

	<i>E. coli</i>	phage λ	<i>V. cholerae</i>
origin DNA	OriC	Ori λ	OriC-I/II
initiator	DnaA	O	DnaA/RctB
helicase	DnaB	DnaB	DnaB
loader	DnaC	P	DciA

429

430 **Table 1.** Molecules involved in various bacterial DNA replication initiation systems.

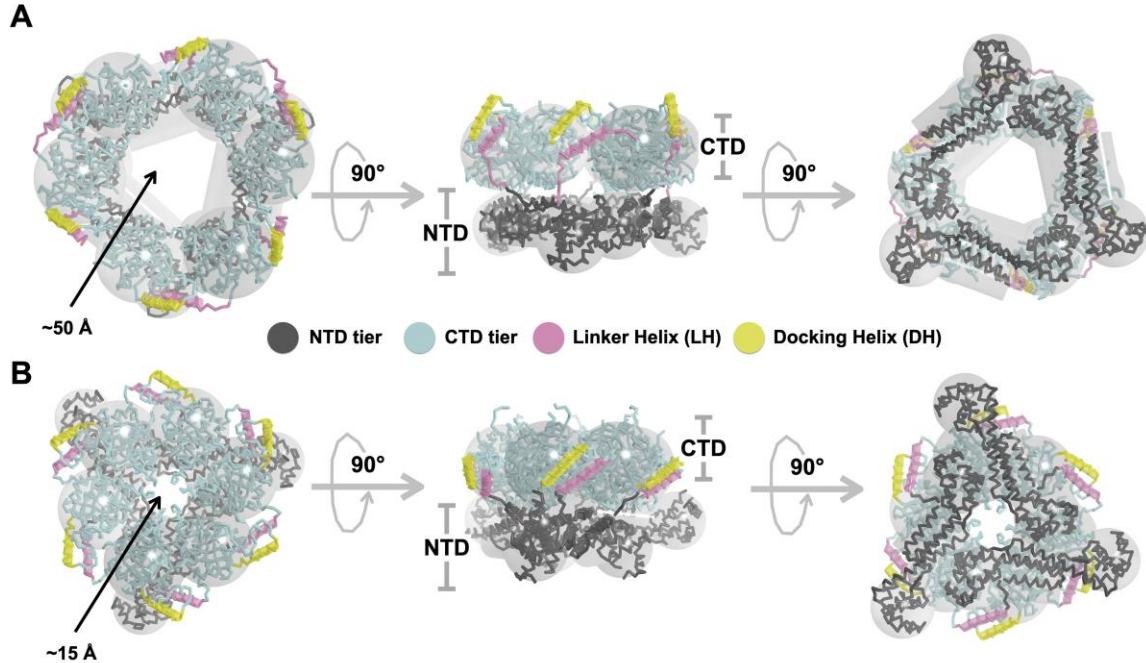
431



432
433
434
435
436
437
438
439
440
441

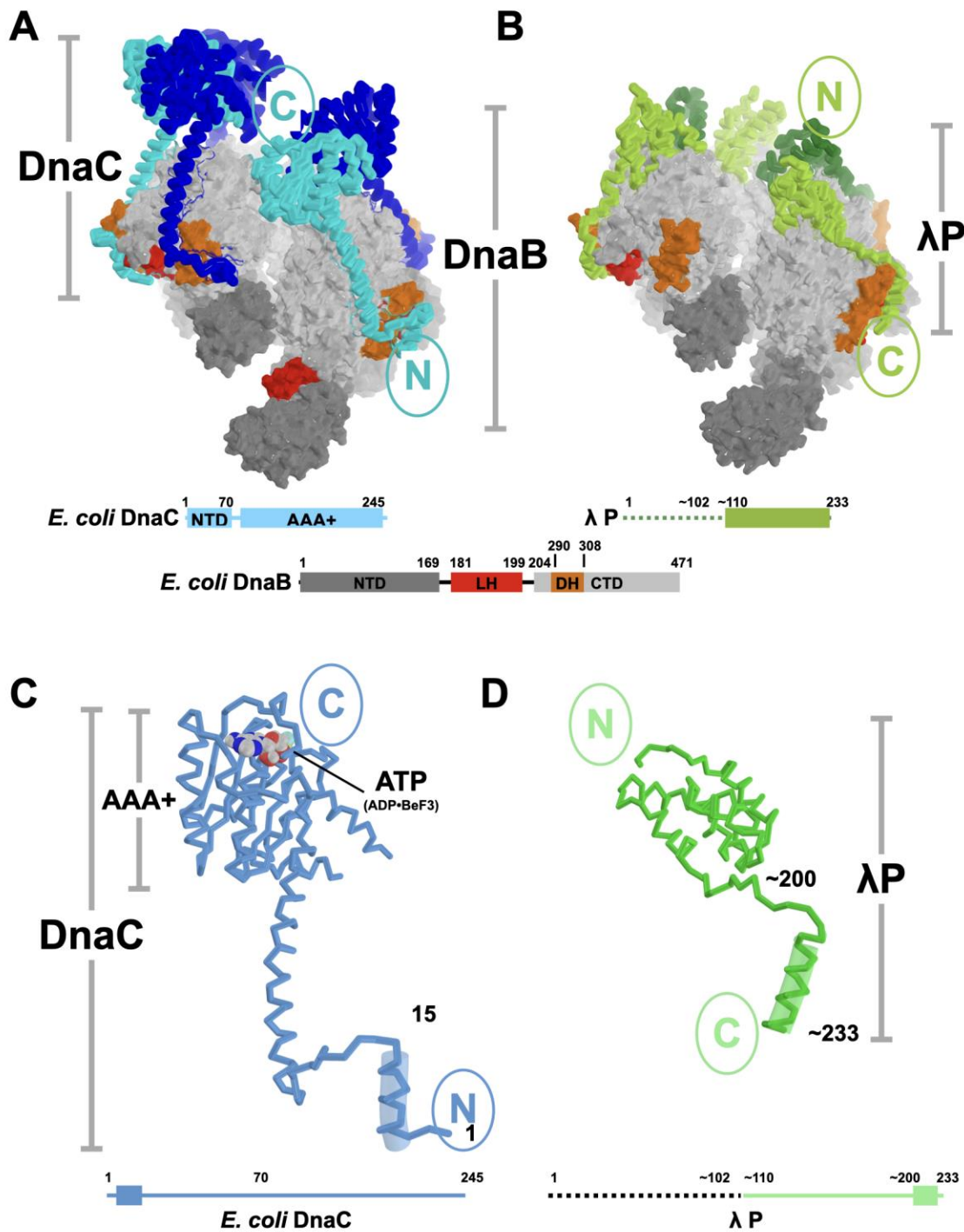
Figure 1. Loading of the Bacterial DnaB Replicative Helicase at a Replication Origin.
 The DnaB loading pathway passes through at least four stages (I, II, III, and IV). DnaB sub-domains are depicted according to their overall shape (amino-terminal domain (NTD): a mushroom-like shape; carboxy-terminal domain (CTD): sphere; both in varying shades of gray). The Linker-Helix (LH, pink) and Docking-Helix (DH, yellow) elements are depicted in a ribbon and transparent cylinder representation. The DnaC helicase loader is shown as a blue ribbon. The DNA strands, one of which is included in the central DnaB chamber, and the second excluded, are colored in chocolate brown and light brown, respectively.

442
443
444
445
446
447



448
449 **Figure 2. Overview of the DnaB replicative helicase.** DnaB adopts at least two distinct
450 configurations, termed dilated (A) and constricted (B) [62–64]. DnaB sub-domains are
451 depicted according to their overall shape (amino-terminal domain (NTD): a mushroom-
452 like shape; carboxy-terminal domain (CTD): sphere; both in varying shades of gray).
453 Superimposed on these shapes of DnaB are ribbon representations, colored in gray and
454 light cyan of the NTD and CTD tiers, respectively, in various poses of the dilated (A, PDB
455 = 2R6A) and constricted (B, PDB = 4NMN) forms of DnaB. The linker and docking helices
456 are depicted as cylinders, and colored pink and yellow, respectively.

457



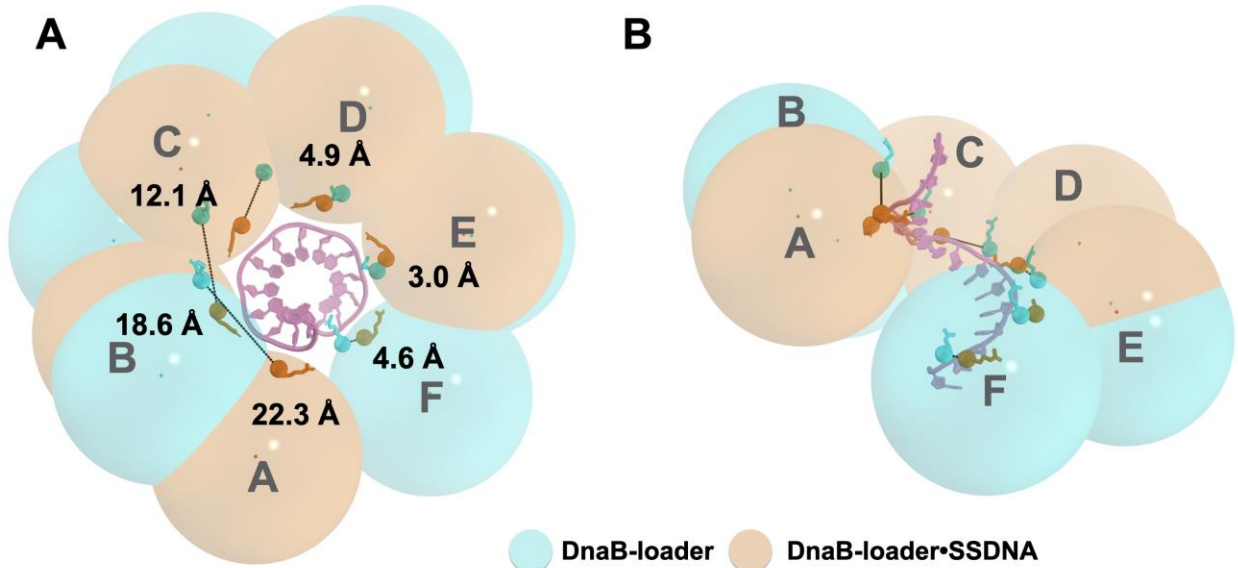
458
459
460
461
462
463

Figure 3. *E. coli* DnaB Complexed with the DnaC (A) and λ P (B) Helicase Loaders.
 Protomers of the DnaC and λ P helicase loaders are colored in alternating shades of blue (DnaC) and green (λ P). The *E. coli* DnaB helicase in each loader complex is represented in a surface rendering, with the amino-terminal domain (NTD) and the carboxy-terminal domain (CTD) layers colored in darker and lighter shades of gray, respectively. Linker-

464 helices (LH) and docking-helices (DH) are in colored in red and orange, respectively. The
465 DnaB hexamers from the loader complexes are superimposed on the CTD of the
466 protomer at the bottom of the spiral in this pose. The primary sequence of each loader
467 and DnaB is represented as a linear schematic, with salient features annotated and
468 colored to match the molecular representations. Only the carboxy terminal domain of λ
469 P was visible in the EM maps of the BP complex (the missing segment is depicted as a
470 dashed line). The terminal helix of each loader (DnaC: N-terminal; λ P: C-terminal) are
471 depicted as ribbons and transparent cylinders. The amino (N) and carboxy (C) termini of
472 each loader is indicated in each panel.

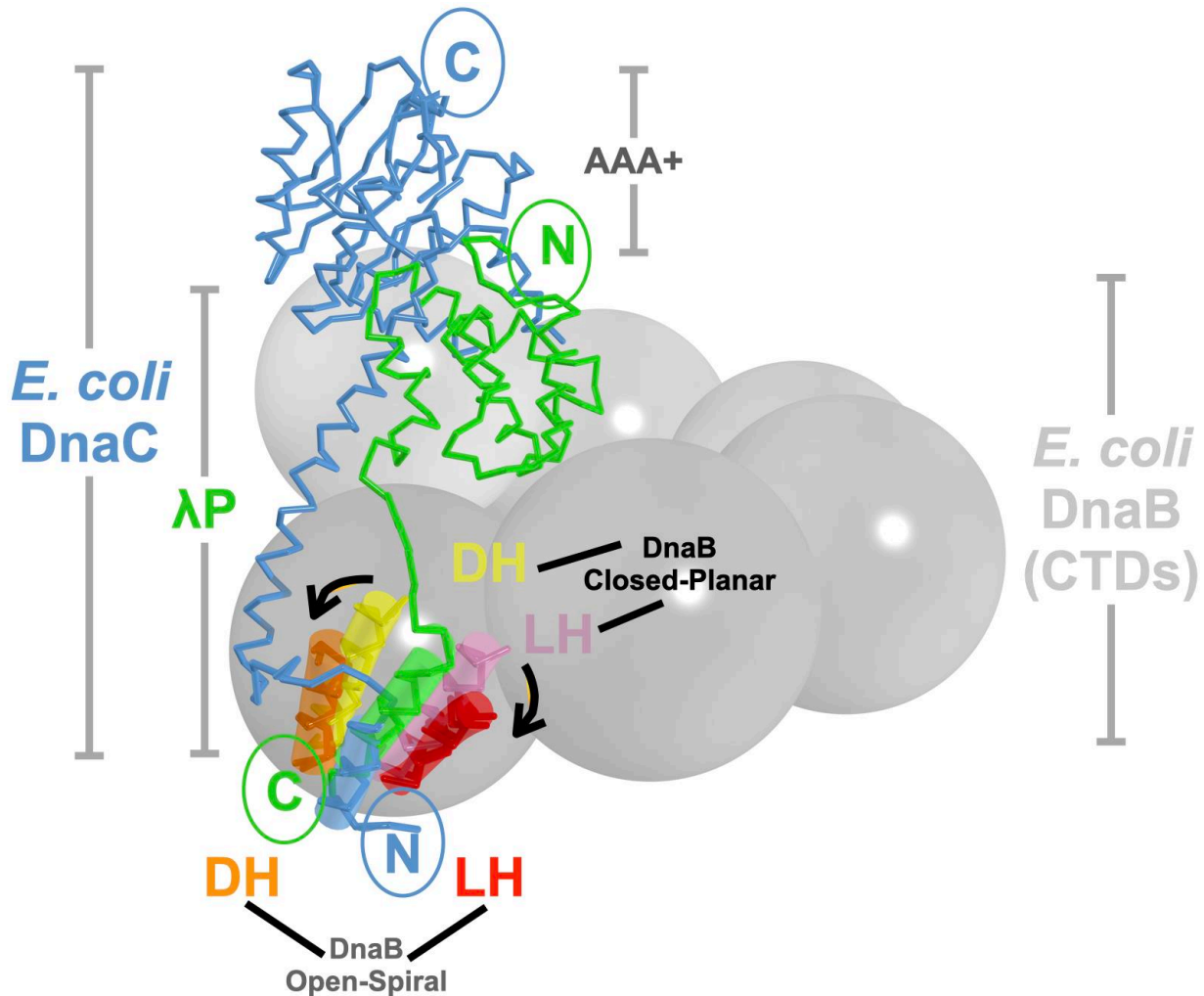
473

474



475
 476 **Figure 4. The ssDNA Binding Site is Altered in the Loader Bound Form of DnaB.**
 477 The BC complex without ssDNA (PDB = 6QEL) was superimposed (RMSD = 0.85 Å) onto
 478 the C-terminal domain of chain F of the ssDNA bound complex (PDB = 6QEM). The large
 479 spheres represent the CTDs of the BC complex with (light brown) and without (cyan)
 480 ssDNA. The alpha carbons of arginine 403, which makes a key contact to ssDNA in the
 481 BC complex, are depicted as smaller spheres for the ssDNA complex (brown) and apo
 482 complex (dark cyan). Distances between the alpha carbons of arginine 403 from
 483 equivalent DnaB subunits are shown. The six chains from the ssDNA-bound complex
 484 are identified by letters (A, B, C, etc.). Poses in panels A and B are related by a 90°
 485 rotation about the horizontal axis.

486
 487



488
489 **Figure 5. Convergent Evolution/Molecular Mimicry in the Mechanism of Opening**
490 **of the *E. coli* DnaB Replicative Helicase by the *E. coli* DnaC and λ P Helicase**
491 **Loaders.** The DnaC and λ P helicase loaders are shown in a ribbon representation,

492 colored light blue (DnaC) and green (λ P), with their respective amino and carboxy termini
493 marked. For clarity, only one copy of each loader is shown. The DnaB hexamer from
494 each loader complex is superimposed on the carboxy-terminal domain (CTD) of the
495 protomer at the bottom of the spiral in this pose; the docking helix element was excluded
496 from the alignment to produce an RMSD of 1.3 Å. For clarity, only the CTD tier of DnaB,
497 represented as a set of spheres, colored in varying shades of gray, is shown. The linker
498 (LH) and docking (DH) helices are depicted as a ribbon and transparent cylinder. The LH
499 and DH from the closed-planar form of DnaB are colored yellow and pink, respectively;
500 the corresponding elements from the DnaC and λ P loader-bound DnaB are in orange
501 and red, respectively. The black arrow signifies direction of motion of the LH and DH
502 elements on binding the DnaC and λ P loaders.

503

504 **References**

505

- 506 1 Yao, N. and O'Donnell, M. (2016) Bacterial and Eukaryotic Replisome Machines. *JSM*
507 *biochemistry and molecular biology* 3,
- 508 2 Yao, N.Y. and O'Donnell, M.E. (2016) Evolution of replication machines. *Critical*
509 *Reviews in Biochemistry and Molecular Biology* 51, 135–149
- 510 3 MacNeill, S.A. (2011) Protein-protein interactions in the archaeal core replisome.
511 *Biochemical Society transactions* 39, 163–168
- 512 4 Kaguni, J.M. (2014) DnaA, DnaB, and DnaC. pp. 1–14, Springer New York
- 513 5 Velten, M. et al. (2003) A Two-Protein Strategy for the Functional Loading of a
514 *Cellular Replicative DNA Helicase*. *Mol Cell* 11, 1009–1020
- 515 6 Brézellec, P. et al. (2016) DciA is an ancestral replicative helicase operator essential
516 for bacterial replication initiation. *Nature communications* 7, 13271
- 517 7 Brézellec, P. et al. (2017) Domestication of lambda phage genes into a putative third
518 type of Replicative Helicase Matchmaker. *Genome Biology and Evolution* 9, 1561–1566
- 519 8 Bleichert, F. et al. (2017) Mechanisms for initiating cellular DNA replication. *Science*
520 355, eaah6317
- 521 9 Marsin, S. et al. (2021) Study of the DnaB:DciA interplay reveals insights into the
522 primary mode of loading of the bacterial replicative helicase. *Nucleic Acids Res* DOI:
523 10.1093/nar/gkab463
- 524 10 Bell, S.P. and Kaguni, J.M. (2013) Helicase loading at chromosomal origins of
525 replication. *Cold Spring Harbor perspectives in biology* 5, a010124
- 526 11 Kaguni, J.M. (2013) DNA Replication: Initiation in Bacteria. pp. 121–125, Elsevier
- 527 12 Chodavarapu, S. and Kaguni, J.M. (2016) Replication Initiation in Bacteria. 39, 1–30
- 528 13 Katayama, T. (2017) Initiation of DNA Replication at the Chromosomal Origin of E.
529 *coli*, *oriC*. *Adv Exp Med Biol* 1042, 79–98
- 530 14 Lewis, J.S. et al. (2016) The *E. coli* DNA Replication Fork. *The Enzymes* 39, 31–88
- 531 15 Mott, M.L. and Berger, J.M. (2007) DNA replication initiation: mechanisms and
532 regulation in bacteria. *Nature Reviews Microbiology* 5, 343–354

- 533 16 Duderstadt, K.E. et al. (2010) Origin remodeling and opening in bacteria rely on
534 distinct assembly states of the DnaA initiator. *The Journal of biological chemistry* 285,
535 28229–28239
- 536 17 Egan, E.S. and Waldor, M.K. (2003) Distinct Replication Requirements for the Two
537 *Vibrio cholerae* Chromosomes. *Cell* 114, 521–530
- 538 18 Orlova, N. et al. (2017) The replication initiator of the cholera pathogen's second
539 chromosome shows structural similarity to plasmid initiators. *Nucleic Acids Res* 45,
540 3724–3737
- 541 19 Leonard, A.C. and Grimwade, J.E. (2015) The orisome: structure and function. *Front*
542 *Microbiol* 6, 545
- 543 20 Wolański, M. et al. (2014) oriC-encoded instructions for the initiation of bacterial
544 chromosome replication. *Frontiers in microbiology* 5, 735
- 545 21 Val, M.E. et al. (2016) A checkpoint control orchestrates the replication of the two
546 chromosomes of *Vibrio cholerae*. *Science Advances* 2, e1501914–e1501914
- 547 22 Val, M.-E. et al. (2014) Management of multipartite genomes: the *Vibrio cholerae*
548 model. *Current Opinion in Microbiology* 22, 120–126
- 549 23 Gerding, M.A. et al. (2015) Molecular Dissection of the Essential Features of the
550 Origin of Replication of the Second *Vibrio cholerae* Chromosome. *mBio* 6,
- 551 24 Fournes, F. et al. (2018) Replicate Once Per Cell Cycle: Replication Control of
552 Secondary Chromosomes. *Frontiers in microbiology* 9, 1833
- 553 25 Martins, F. de L. et al. (2018) *Vibrio cholerae* chromosome 2 copy number is
554 controlled by the methylation-independent binding of its monomeric initiator to the
555 chromosome 1 crtS site. *Nucleic Acids Research* 81, e00019-17–12
- 556 26 Konieczny, I. et al. (2014) Iteron Plasmids. *Microbiology Spectrum* 2,
- 557 27 Weigel, C. and Seitz, H. (2006) Bacteriophage replication modules. *FEMS*
558 *microbiology reviews* 30, 321–381
- 559 28 Trojanowski, D. et al. (2018) Where and When Bacterial Chromosome Replication
560 Starts: A Single Cell Perspective. *Front Microbiol* 9, 2819
- 561 29 Luo, H. et al. (2018) Recent development of Ori-Finder system and DoriC database
562 for microbial replication origins. *Brief Bioinform* 20, 1114–1124
- 563 30 Kohiyama, M. (2020) Research on DnaA in the early days. *Res Microbiol* 171, 287–
564 289

- 565 31 Leonard, A.C. et al. (2019) Changing Perspectives on the Role of DnaA-ATP in
566 Orisome Function and Timing Regulation. *Front Microbiol* 10, 2009
- 567 32 Hansen, F.G. and Atlung, T. (2018) The DnaA Tale. *Front Microbiol* 9, 319
- 568 33 Egan, E.S. and Waldor, M.K. (2003) Distinct replication requirements for the two
569 *Vibrio cholerae* chromosomes. *Cell* 114, 521–530
- 570 34 Chatterjee, S. et al. (2020) Interactions of replication initiator RctB with single- and
571 double-stranded DNA in origin opening of *Vibrio cholerae* chromosome 2. *Nucleic Acids*
572 *Res* DOI: 10.1093/nar/gkaa826
- 573 35 Ramachandran, R. et al. (2018) Chromosome 1 licenses chromosome 2 replication
574 in *Vibrio cholerae* by doubling the crtS gene dosage. *PLoS genetics* 14, e1007426
- 575 36 Jha, J.K. et al. (2014) Initiator protein dimerization plays a key role in replication
576 control of *Vibrio cholerae* chromosome 2. *Nucleic Acids Research* 42, 10538–10549
- 577 37 Fournes, F. et al. (2021) The coordinated replication of *Vibrio cholerae*'s two
578 chromosomes required the acquisition of a unique domain by the RctB initiator. *Nucleic*
579 *Acids Res* 49, 11119–11133
- 580 38 Wegrzyn, K.E. et al. (2016) Replisome Assembly at Bacterial Chromosomes and
581 Iteron Plasmids. *Frontiers in molecular biosciences* 3, 617
- 582 39 Wawrzycka, A. et al. (2015) Plasmid replication initiator interactions with origin 13-
583 mers and polymerase subunits contribute to strand-specific replisome assembly. *Proc*
584 *National Acad Sci* 112, E4188–E4196
- 585 40 Konieczny, I. et al. (2014) Iteron Plasmids. *Microbiol Spectr* 2,
- 586 41 Wickner, S. and McKenney, K. (1987) Deletion analysis of the DNA sequence
587 required for the in vitro initiation of replication of bacteriophage lambda. *The Journal of*
588 *biological chemistry* 262, 13163–13167
- 589 42 Wold, M.S. et al. (1982) Initiation of bacteriophage lambda DNA replication in vitro
590 with purified lambda replication proteins. *Proceedings of the National Academy of*
591 *Sciences of the United States of America* 79, 6176–6180
- 592 43 Alfano, C. and McMacken, R. (1989) Ordered assembly of nucleoprotein structures
593 at the bacteriophage lambda replication origin during the initiation of DNA replication.
594 *The Journal of biological chemistry* 264, 10699–10708
- 595 44 Mensa-Wilmot, K. et al. (1989) Reconstitution of a nine-protein system that initiates
596 bacteriophage lambda DNA replication. *The Journal of biological chemistry* 264, 2853–
597 2861

- 598 45 Dodson, M. et al. (1989) Specialized nucleoprotein structures at the origin of
599 replication of bacteriophage lambda. Protein association and disassociation reactions
600 responsible for localized initiation of replication. *The Journal of biological chemistry* 264,
601 10719–10725
- 602 46 Dodson, M. et al. (1985) Specialized nucleoprotein structures at the origin of
603 replication of bacteriophage lambda: complexes with lambda O protein and with lambda
604 O, lambda P, and *Escherichia coli* DnaB proteins. *Proceedings of the National Academy
605 of Sciences of the United States of America* 82, 4678–4682
- 606 47 Dodson, M. et al. (1986) Specialized nucleoprotein structures at the origin of
607 replication of bacteriophage lambda: localized unwinding of duplex DNA by a six-protein
608 reaction. *Proceedings of the National Academy of Sciences of the United States of
609 America* 83, 7638–7642
- 610 48 LeBowitz, J.H. and McMacken, R. (1984) The bacteriophage lambda O and P
611 protein initiators promote the replication of single-stranded DNA. *Nucleic Acids
612 Research* 12, 3069–3088
- 613 49 Roberts, J.D. and McMacken, R. (1983) The bacteriophage lambda O replication
614 protein: isolation and characterization of the amplified initiator. *Nucleic Acids Research*
615 11, 7435–7452
- 616 50 O'Donnell, M.E. and Li, H. (2018) The ring-shaped hexameric helicases that function
617 at DNA replication forks. *Nat Struct Mol Biol* 25, 122–130
- 618 51 Galletto, R. and Bujalowski, W. (2002) The *E. coli* replication factor DnaC protein
619 exists in two conformations with different nucleotide binding capabilities. I.
620 Determination of the binding mechanism using ATP and ADP fluorescent analogues.
621 *Biochemistry* 41, 8907–8920
- 622 52 Davey, M.J. et al. (2002) The DnaC helicase loader is a dual ATP/ADP switch
623 protein. *The EMBO journal* 21, 3148–3159
- 624 53 Mott, M.L. et al. (2008) Structural synergy and molecular crosstalk between bacterial
625 helicase loaders and replication initiators. *Cell* 135, 623–634
- 626 54 Galletto, R. et al. (2004) Global conformation of the *Escherichia coli* replication factor
627 DnaC protein in absence and presence of nucleotide cofactors. *Biochemistry* 43,
628 10988–11001
- 629 55 Felczak, M.M. et al. (2017) DnaC, the indispensable companion of DnaB helicase,
630 controls the accessibility of DnaB helicase by primase. *The Journal of biological
631 chemistry* 292, 20871–20882

- 632 56 Learn, B.A. et al. (1997) Cryptic single-stranded-DNA binding activities of the phage
633 lambda P and Escherichia coli DnaC replication initiation proteins facilitate the transfer
634 of E. coli DnaB helicase onto DNA. *Proceedings of the National Academy of Sciences*
635 of the United States of America
- 636 57 Stephens, K.M. and McMacken, R. (1997) Functional properties of replication fork
637 assemblies established by the bacteriophage lambda O and P replication proteins. *The*
638 *Journal of biological chemistry* 272, 28800–28813
- 639 58 Mallory, J.B. et al. (1990) Host virus interactions in the initiation of bacteriophage
640 lambda DNA replication. Recruitment of Escherichia coli DnaB helicase by lambda P
641 replication protein. *The Journal of biological chemistry* 265, 13297–13307
- 642 59 Alfano, C. and McMacken, R. (1989) Heat shock protein-mediated disassembly of
643 nucleoprotein structures is required for the initiation of bacteriophage lambda DNA
644 replication. *The Journal of biological chemistry* 264, 10709–10718
- 645 60 Bleichert, F. (2019) Mechanisms of replication origin licensing: a structural
646 perspective. *Curr Opin Struc Biol* 59, 195–204
- 647 61 Kaguni, J.M. (2018) The Macromolecular Machines that Duplicate the Escherichia
648 coli Chromosome as Targets for Drug Discovery. *Antibiotics* 7, 23
- 649 62 Wang, G. et al. (2008) The structure of a DnaB-family replicative helicase and its
650 interactions with primase. *Nat Struct Mol Biol* 15, 94–100
- 651 63 Strychar ska, M.S. et al. (2013) Nucleotide and partner-protein control of bacterial
652 replicative helicase structure and function. *Molecular Cell* 52, 844–854
- 653 64 Bailey, S. et al. (2007) Structure of hexameric DnaB helicase and its complex with a
654 domain of DnaG primase. *Science (New York, NY)* 318, 459–463
- 655 65 Arias-Palomo, E. et al. (2019) Physical Basis for the Loading of a Bacterial
656 Replicative Helicase onto DNA. *Mol Cell* 74, 173–184.e4
- 657 66 Arias-Palomo, E. et al. (2013) The Bacterial DnaC Helicase Loader Is a DnaB Ring
658 Breaker. *Cell* 153, 438–448
- 659 67 Itsathitphaisarn, O. et al. (2012) The hexameric helicase DnaB adopts a nonplanar
660 conformation during translocation. *Cell* 151, 267–277
- 661 68 Chase, J. et al. (2018) Mechanisms of opening and closing of the bacterial
662 replicative helicase. *Elife* 7, 1822

- 663 69 Marszalek, J. et al. (1996) Domains of DnaA protein involved in interaction with
664 DnaB protein, and in unwinding the *Escherichia coli* chromosomal origin. *The Journal of*
665 *biological chemistry* 271, 18535–18542
- 666 70 Marszalek, J. and Kaguni, J.M. (1994) DnaA protein directs the binding of DnaB
667 protein in initiation of DNA replication in *Escherichia coli*. *The Journal of biological*
668 *chemistry* 269, 4883–4890
- 669 71 Sutton, M.D. et al. (1998) *Escherichia coli* DnaA protein. The N-terminal domain and
670 loading of DnaB helicase at the *E. coli* chromosomal origin. *The Journal of biological*
671 *chemistry* 273, 34255–34262
- 672 72 Davey, M.J. and O'Donnell, M. (2003) Replicative helicase loaders: ring breakers
673 and ring makers. *Current biology* : CB 13, R594-6
- 674 73 Kornberg, A. and Baker, T.A. (2005) *DNA Replication*, University Science Books.
- 675 74 Chodavarapu, S. et al. (2015) DnaC traps DnaB as an open ring and remodels the
676 domain that binds primase. *Nucleic Acids Research* DOI: 10.1093/nar/gkv961
- 677 75 Davey, M.J. et al. (2002) Motors and switches: AAA+ machines within the replisome.
678 *Nature Reviews Molecular Cell Biology* 3, 826–835
- 679 76 Wahle, E. et al. (1989) The dnaB-dnaC replication protein complex of *Escherichia*
680 *coli*. I. Formation and properties. *The Journal of biological chemistry* 264, 2463–2468
- 681 77 Wahle, E. et al. (1989) The dnaB-dnaC replication protein complex of *Escherichia*
682 *coli*. II. Role of the complex in mobilizing dnaB functions. *The Journal of biological*
683 *chemistry* 264, 2469–2475
- 684 78 Biswas, S.B. and Biswas, E.E. (1987) Regulation of Dnab Function in Dna-
685 Replication in *Escherichia-Coli* by Dnac and Lambda-P Gene-Products. *The Journal of*
686 *biological chemistry* 262, 7831–7838
- 687 79 Puri, N. et al. (2021) The molecular coupling between substrate recognition and ATP
688 turnover in a AAA+ hexameric helicase loader. *Elife* 10, e64232
- 689 80 Sandler, S.J. (2005) Requirements for Replication Restart Proteins During
690 Constitutive Stable DNA Replication in *Escherichia coli* K-12. *Genetics* 169, 1799–1806
- 691 81 Michel, B. and Sandler, S.J. (2017) Replication Restart in Bacteria. *J Bacteriol* 199,
692 e00102-17
- 693 82 Michel, B. et al. (2018) Replication Fork Breakage and Restart in *Escherichia coli*.
694 *Microbiol Mol Biol R* 82, e00013-18

- 695 83 Nagata, K. et al. (2019) Crystal structure of the complex of the interaction domains of
696 E. coli DnaB helicase and DnaC helicase loader: Structural basis implying a distortion-
697 accumulation mechanism for the DnaB ring opening caused by DnaC binding. *Journal
698 of biochemistry* 5, a010108
- 700 84 Bruand, C. et al. (2005) Functional interplay between the *Bacillus subtilis* DnaD and
701 DnaB proteins essential for initiation and re-initiation of DNA replication. *Molecular
Microbiology* 55, 1138–1150
- 702 85 Ioannou, C. et al. (2006) Helicase binding to DnaI exposes a cryptic DNA-binding
703 site during helicase loading in *Bacillus subtilis*. *Nucleic Acids Research* 34, 5247–5258
- 704 86 Duderstadt, K.E. and Berger, J.M. (2013) A structural framework for replication origin
705 opening by AAA+ initiation factors. *Current Opinion in Structural Biology* 23, 144–153
- 706 87 Gates, S.N. and Martin, A. (2019) Stairway to translocation: AAA+ motor structures
707 reveal the mechanisms of ATP-dependent substrate translocation. *Protein science : a
708 publication of the Protein Society* DOI: 10.1002/pro.3743
- 709 88 Miller, J.M. and Enemark, E.J. (2016) Fundamental Characteristics of AAA+ Protein
710 Family Structure and Function. *Archaea* (Vancouver, BC) 2016, 9294307
- 711 89 Duderstadt, K.E. and Berger, J.M. (2008) AAA+ ATPases in the Initiation of DNA
712 Replication. *Crit Rev Biochem Mol* 43, 163–187
- 713 90 Greci, M.D. and Bell, S.D. (2020) Archaeal DNA Replication. *Annu Rev Microbiol* 74,
714 1–16
- 715 91 Kelman, L.M. et al. (2020) Unwinding 20 Years of the Archaeal Minichromosome
716 Maintenance Helicase. *J Bacteriol* 202,
- 717 92 Bai, L. et al. (2017) DNA Replication, From Old Principles to New Discoveries.
718 *Advances in experimental medicine and biology* 1042, 207–228
- 719 93 Wiegand, T. et al. (2019) The conformational changes coupling ATP hydrolysis and
720 translocation in a bacterial DnaB helicase. *Nat Commun* 10, 31
- 721 94 Kelch, B.A. (2016) Review: The lord of the rings: Structure and mechanism of the
722 sliding clamp loader. *Biopolymers* 105, 532–546
- 723 95 Kelch, B.A. et al. (2011) How a DNA polymerase clamp loader opens a sliding
724 clamp. *Science* (New York, NY) 334, 1675–1680
- 725 96 Simonetta, K.R. et al. (2009) The mechanism of ATP-dependent primer-template
726 recognition by a clamp loader complex. *Cell* 137, 659–671

- 727 97 Bowman, G.D. et al. (2004) Structural analysis of a eukaryotic sliding DNA clamp–
728 clamp loader complex. *Nature* 429, 724–730
- 729 98 Erzberger, J.P. and Berger, J.M. (2006) Evolutionary relationships and structural
730 mechanisms of AAA+ proteins. *Annual Review of Biophysics and Biomolecular
731 Structure* 35, 93–114
- 732 99 Khan, Y.A. et al. (2021) The AAA+ superfamily: a review of the structural and
733 mechanistic principles of these molecular machines. *Crit Rev Biochem Mol* DOI:
734 10.1080/10409238.2021.1979460
- 735 100 Puchades, C. et al. (2020) The molecular principles governing the activity and
736 functional diversity of AAA+ proteins. *Nat Rev Mol Cell Bio* 21, 43–58
- 737 101 Makowska-Grzyska, M. and Kaguni, J.M. (2010) Primase directs the release of
738 DnaC from DnaB. *Molecular Cell* 37, 90–101
- 739 102 Costantino, D. et al. (2008) tRNA-mRNA mimicry drives translation initiation from a
740 viral IRES. *Nature Structural & Molecular Biology* 15, 57–64
- 741 103 Ryckelynck, M. et al. (2005) tRNAs and tRNA mimics as cornerstones of
742 aminoacyl-tRNA synthetase regulations. *Biochimie* 87, 835–845
- 743 104 Nakamura, Y. and Ito, K. (2011) tRNA mimicry in translation termination and
744 beyond. *Wiley Interdisciplinary Reviews: RNA* 2, 647–668
- 745 105 Liu, D. et al. (1998) Solution structure of a TBP-TAF(II)230 complex: protein
746 mimicry of the minor groove surface of the TATA box unwound by TBP. *Cell* 94, 573–
747 583
- 748 106 Riedl, S.J. et al. (2001) Structural Basis for the Inhibition of Caspase-3 by XIAP.
749 *Cell* 104, 1–10
- 750 107 Pahari, S. et al. (2017) Morbid Sequences Suggest Molecular Mimicry between
751 Microbial Peptides and Self-Antigens: A Possibility of Inciting Autoimmunity. *Frontiers in
752 microbiology* 8, 392
- 753 108 Chemes, L.B. et al. (2015) Convergent evolution and mimicry of protein linear
754 motifs in host-pathogen interactions. *Current Opinion in Structural Biology* 32, 91–101
- 755 109 Drayman, N. et al. (2013) Pathogens Use Structural Mimicry of Native Host Ligands
756 as a Mechanism for Host Receptor Engagement. *Cell host & microbe* 14, 63–73
- 757 110 Lasso, G. et al. (2020) A Sweep of Earth’s Virome Reveals Host-Guided Viral
758 Protein Structural Mimicry and Points to Determinants of Human Disease. *Cell Syst* 12,
759 82–91.e3

- 760 111 Wucherpfennig, K.W. and Strominger, J.L. (1995) Molecular mimicry in T cell-
761 mediated autoimmunity: Viral peptides activate human T cell clones specific for myelin
762 basic protein. *Cell* 80, 695–705
- 763 112 Grimwade, J.E. and Leonard, A.C. (2021) Blocking, Bending, and Binding:
764 Regulation of Initiation of Chromosome Replication During the *Escherichia coli* Cell
765 Cycle by Transcriptional Modulators That Interact With Origin DNA. *Front Microbiol* 12,
766 732270
- 767 113 Zhai, Y. and Tye, B.-K. (2017) Structure of the MCM2-7 Double Hexamer and Its
768 Implications for the Mechanistic Functions of the Mcm2-7 Complex. *Adv Exp Med Biol*
769 1042, 189–205
- 770 114 Fernandez, A.J. and Berger, J.M. (2021) Mechanisms of hexameric helicases. *Crit
771 Rev Biochem Mol* DOI: 10.1080/10409238.2021.1954597
- 772 115 Yuan, Z. et al. (2020) Structural mechanism of helicase loading onto replication
773 origin DNA by ORC-Cdc6. *Proc National Acad Sci* DOI: 10.1073/pnas.2006231117
- 774 116 Yuan, Z. et al. (2020) DNA unwinding mechanism of a eukaryotic replicative CMG
775 helicase. *Nat Commun* 11, 688
- 776 117 Langston, L.D. and O'Donnell, M.E. (2019) An explanation for origin unwinding in
777 eukaryotes. *Elife* 8, e46515
- 778 118 Yuan, Z. et al. (2018) Structure of Eukaryotic CMG Helicase at a Replication Fork
779 and Implications for Replisome Architecture and Origin Initiation. *Faseb J* 32, 646.7-
780 646.7
- 781 119 Koonin, E.V. (1993) A common set of conserved motifs in a vast variety of putative
782 nucleic acid-dependent ATPases including MCM proteins involved in the initiation of
783 eukaryotic DNA replication. *Nucleic Acids Research* 21, 2541–2547
- 784 120 Iyer, L.M. et al. (2004) Evolutionary history and higher order classification of AAA+
785 ATPases. *J Struct Biol* 146, 11–31
- 786 121 Leipe, D.D. et al. (2000) The bacterial replicative helicase DnaB evolved from a
787 RecA duplication. *Genome Research* 10, 5–16
- 788 122 Leipe, D.D. et al. (1999) Did DNA replication evolve twice independently? *Nucleic
789 Acids Res* 27, 3389–3401
- 790 123 Leipe, D.D. et al. (2003) Evolution and Classification of P-loop Kinases and Related
791 Proteins. *J Mol Biol* 333, 781–815

- 792 124 Kowalski, D. and Eddy, M.J. (1989) The DNA unwinding element: a novel, cis-
793 acting component that facilitates opening of the *Escherichia coli* replication origin. *The*
794 *EMBO journal* 8, 4335–4344
- 795 125 Richardson, T.T. et al. (2016) The bacterial DnaA-trio replication origin element
796 specifies ssDNA initiator binding. *Nature* 534, 412–416
- 797 126 Spinks, R.R. et al. (2021) Single-Molecule Insights Into the Dynamics of Replicative
798 Helicases. *Frontiers Mol Biosci* 8, 741718
- 799 127 Lo, C.-Y. and Gao, Y. (2021) DNA Helicase-Polymerase Coupling in Bacteriophage
800 DNA Replication. *Viruses* 13, 1739
- 801 128 Li, H. et al. (2020) Anatomy of a twin DNA replication factory. *Biochem Soc T* 48,
802 2769–2778
- 803 129 Yao, N.Y. and O'Donnell, M.E. (2020) The DNA Replication Machine: Structure and
804 Dynamic Function. *Subcell Biochem* 96, 233–258
- 805 130 Rousseau, F. et al. (2012) Implications of 3D domain swapping for protein folding,
806 misfolding and function. *Adv Exp Med Biol* 747, 137–152
- 807 131 Rousseau, F. et al. (2003) The unfolding story of three-dimensional domain
808 swapping. *Structure* 11, 243–251
- 809 132 Newcomer, M.E. (2002) Protein folding and three-dimensional domain swapping: a
810 strained relationship? *Curr Opin Struc Biol* 12, 48–53
- 811 133 Bennett, M.J. et al. (1995) 3D domain swapping: a mechanism for oligomer
812 assembly. *Protein Sci* 4, 2455–2468
- 813 134 Schlunegger, M.P. et al. (1997) Oligomer formation by 3D domain swapping: a
814 model for protein assembly and misassembly. *Adv Protein Chem* 50, 61–122
- 815 135 Hakansson, M. and Linse, S. (2002) Protein reconstitution and 3D domain
816 swapping. *Curr Protein Pept Sc* 3, 629–642
- 817 136 Aravind, L. et al. (2004) A novel family of P-loop NTPases with an unusual phyletic
818 distribution and transmembrane segments inserted within the NTPase domain. *Genome*
819 *Biol* 5, R30
- 820 137 Leipe, D.D. et al. (2002) Classification and evolution of P-loop GTPases and related
821 ATPases11Edited by J. Thornton. *J Mol Biol* 317, 41–72
- 822 138 Longo, L.M. et al. (2020) On the emergence of P-Loop NTPase and Rossmann
823 enzymes from a Beta-Alpha-Beta ancestral fragment. *Elife* 9, e64415

- 824 139 Walker, J.E. et al. (1982) Distantly related sequences in the alpha- and beta-
825 subunits of ATP synthase, myosin, kinases and other ATP-requiring enzymes and a
826 common nucleotide binding fold. *Embo J* 1, 945–951
- 827 140 Saraste, M. et al. (1990) The P-loop — a common motif in ATP- and GTP-binding
828 proteins. *Trends Biochem Sci* 15, 430–434
- 829 141 Neuwald, A.F. et al. (1999) AAA+: A class of chaperone-like ATPases associated
830 with the assembly, operation, and disassembly of protein complexes. *Genome*
831 *Research* 9, 27–43
- 832 142 Jez, J.M. (2017) Revisiting protein structure, function, and evolution in the genomic
833 era. *J Invertebr Pathol* 142, 11–15
- 834 143 Theobald, D.L. and Wuttke, D.S. (2005) Divergent Evolution Within Protein
835 Superfolds Inferred from Profile-based Phylogenetics. *J Mol Biol* 354, 722–737
- 836 144 Stebbins, C.E. and Galán, J.E. (2001) Structural mimicry in bacterial virulence.
837 *Nature* 412, 701–705
- 838